

**Design of a Chemical Sampling and Analysis
System Using Excimer Laser Ablation and Quartz
Microcolumns**

by

Luis G. Ortiz

S.B., Mechanical Engineering (1995)
Massachusetts Institute of Technology

Submitted to the Department of Mechanical Engineering
in partial fulfillment of the requirements for the degree of

Master of Science in Mechanical Engineering

at the

MASSACHUSETTS INSTITUTE OF TECHNOLOGY

June 1997

© Massachusetts Institute of Technology 1997. All rights reserved.

Author
Department of Mechanical Engineering
May 9, 1997

Certified by
Kamal Youcef-Toumi
Associate Professor of Mechanical Engineering
Thesis Supervisor

Certified by
Ian W. Hunter
Professor of Mechanical Engineering
Thesis Supervisor

Accepted by
Ain Sonin
Chairman, Departmental Committee on Graduate Students

MASSACHUSETTS INSTITUTE OF TECHNOLOGY

JUL 21 1997

Eng.

Design of a Chemical Sampling and Analysis System Using Excimer Laser Ablation and Quartz Microcolumns

by

Luis G. Ortiz

S.B., Mechanical Engineering (1995)

Massachusetts Institute of Technology

Submitted to the Department of Mechanical Engineering
on May 9, 1997, in partial fulfillment of the
requirements for the degree of
Master of Science in Mechanical Engineering

Abstract

The advent of miniaturization technology has greatly increased the potential for smaller, better performance, and versatile chemical sampling and analysis devices. To this end, a device which can sample and analyze high molecular weight compounds is being developed. In order to make the device as non-invasive as possible, the possibility of using miniaturization technology is being investigated. This will allow for a self-contained system with minimum interaction with the environment. The goal of this thesis was to develop some of the essential tools to realize such a device. First, the ability to sample and analyze high molecular weight compounds using excimer laser ablation and gas chromatography was investigated. Second, a quartz micro-column manufacturing technique which uses a linear Lorentz-force actuator and a carbon dioxide laser to draw quartz micro-columns was developed. Results showed that excimer laser pulse frequency, sample volume and ablation time affected the analytical results in terms of the number of ablation products and their concentration. These results are promising in terms of developing an excimer laser sampling and analysis tool for chemical compounds. The quartz micro-column manufacturing technique developed succeeded in making a few quartz micro-columns which could also find many potential uses. This work lays the foundation which should contribute towards the endgoal of developing a microanalyzer as well as other applications.

Thesis Supervisor: Kamal Youcef-Toumi
Title: Associate Professor of Mechanical Engineering

Thesis Supervisor: Ian W. Hunter
Title: Professor of Mechanical Engineering

Acknowledgments

First of all, I would like to thank Professors Kamal Youcef-Toumi and Ian W. Hunter for giving me the opportunity to work with them in this project. I am truly indebted to them. They provided me with the guidance and encouragement throughout the duration of my graduate studies at MIT and they are truly very admirable, kind people. Furthermore, I would like to thank the many sponsors of the Total Home Automation and Eldercare Systems Consortium who helped fund my education and project.

I also want to give my thanks to all of my labmates whose friendship and helpfulness allowed me to finish my work and to stay sane. In particular, I'd like to thank John Madden for all of his time and help throughout the duration of this project; Peter Madden for showing me how to use the CNC machining center, giving me suggestions on how to design the gas-collection cell, and for the many times he answered my questions; Justin Won for lending me his laptop with which I wrote all of this thesis, and for helping me time and time again with computer problems including setting up software to listen to U2; James for his friendship, continuous encouragement, and help; Joe for his many stories and help; Benjie for his comic relief and encouragement; Colin Brennan for his help and suggestions; Serge for his resourcefulness; Tania for helping me find chemicals for calibration; Susan for her help with administrative matters; and to everyone else in the lab who made it worthwhile: Michel, Debo, Ari, Paul, Mark, and Sylvan.

I want to thank my family and friends who have always supported me throughout these years. In particular, I want to thank my mother and father (Irma and Noris), my three brothers (Gustavo, Victor, and Fito), my two sisters-in-law (Brenda and Angelica) and my two beautiful nieces (Angelica and Liliana). Last but not least, I want to thank my fiancée and future wife Anna for all of her love, inspiration and encouragement. Anna, te amo con todo mi corazon y gracias por todo. Finally, I want to thank God for his help throughout my years at MIT, his guidance and for giving me all of these opportunities.

Contents

1	Introduction	14
1.1	Overview of Chemical Analysis Technology	15
1.1.1	Thermal Sensors	16
1.1.2	Mass Sensors	17
1.1.3	Electrochemical Sensors	18
1.1.4	Optical Sensors	20
1.2	Gas-Liquid Chromatography	27
1.3	Applications for Chemical Analyzers	28
1.3.1	Home	28
1.3.2	Healthcare	28
1.3.3	Environmental	28
1.3.4	Automotive and Defense	29
1.3.5	Other Applications for Chemical Sensors	29
1.4	Motivation for Micro-analyzer Development	30
1.4.1	Lower-End Sensor Technology Problems	31
1.4.2	Thesis Overview	32
2	Gas Chromatography	33
2.1	Introduction	33
2.1.1	Classification of Chromatography	35
2.1.2	Chromatograms	35
2.2	Migration Rates of Solutes	36
2.2.1	Partition Ratios	37

2.2.2	Retention Times	37
2.2.3	The Retention Time and Partition Ratio Relationship	38
2.2.4	The Rate of Migration of Solutes: The Capacity Factor	39
2.2.5	Differential Migration Rates: Selectivity Factor	40
2.3	Band Shapes and Band Broadening	40
2.3.1	The Shapes of Chromatographic Peaks	41
2.3.2	Efficiency of Chromatographic Columns	41
2.3.3	The Plate Height and Band Broadening Relationship	41
2.3.4	Experimental Evaluation of N and H	42
2.4	Variables That Affect Column Efficiency	43
2.4.1	The Effect of Mobile-Phase Flow Rate	44
2.4.2	A Theory of Band Broadening	45
2.5	Column Resolution	49
2.5.1	The Relationship Between Resolution and Properties of the Column and Solute	50
2.5.2	The Relationship Between Resolution and Elution Time	50
2.5.3	Optimization Techniques	50
2.6	The General Elution Problem	51
2.7	Components of a Chromatography System	52
2.8	Applications of Chromatography	53
2.8.1	Qualitative	53
2.8.2	Quantitative	53
2.9	Micro-Chromatographs	54
3	Excimer Laser Ablation	56
3.1	Introduction	56
3.2	Excimer Lasers	56
3.3	Excimer Laser Materials Processing	57
3.3.1	Physical Mechanisms of Ablation	58
3.3.2	Excimer Laser Ablation Product Analysis	59

3.4	Application Areas	60
4	Manufacturing of Quartz Micro-Columns	64
4.1	Introduction	64
4.2	Lorentz Linear Actuator	65
4.3	Amplifier Circuit.	66
4.4	CO_2 Laser Setup and Optics	68
4.5	Quartz As a Column Material	68
4.6	Manufacturing of Quartz Micro-columns	70
5	Excimer Laser Ablation Product Sampling and Analysis	71
5.1	Introduction	71
5.2	Excimer Laser and Optics	71
5.3	Gas Collection Cell	72
5.4	Gas Chromatograph	73
5.5	Excimer Laser Ablation Experiments	73
5.5.1	Influence of Pulse Rate	74
5.5.2	Influence of Injection Volume	74
5.5.3	Influence of Ablation Time	75
5.5.4	Variation According to Material	75
5.5.5	Calibration of Gas Chromatograph	75
6	Results	76
6.1	Quartz Micro-Column Manufacturing	76
6.2	Excimer Laser Ablation Products Sampling and Analysis	78
6.2.1	General Results	78
6.2.2	Influence of Repetition Rate on Concentration	83
6.2.3	Influence of Injection Volume on Concentration	83
6.2.4	Influence of Ablation Time on Concentration	84
6.2.5	Variation According to Material	84
6.2.6	Identification of Ablation Products	85

7 Conclusion and Recommendations	92
7.1 Recommendations	93
7.1.1 Micro-column Manufacturing	93
7.1.2 Excimer Laser Ablation Experiments	94
7.2 Possible Applications	94
7.3 Conclusion	95
A Gas-Collection Cell Drawing	96
B Amplifier Circuit Diagram	99
C Gas Chromatography Setpoints	100
D Integration Results	103
Bibliography	108

List of Figures

1-1	Block diagram for gas/liquid microanalyzer.	15
1-2	General schematic of a thermal catalytic sensor.	16
1-3	Schematic of a SAW sensor with transmitter T, receiver R, and the chemically selective layer deposited on the delay line.	18
1-4	Operation of the tin-oxide sensor.	19
1-5	General arrangement of a spectroscopic absorption/emission experiment. Cuvette of a defined path length L contains solution of concentration C. The single wavelength radiation (λ_A) irradiates the sample and the attenuated radiation or secondary radiation (λ_F) are used to evaluate the extent of the interaction. The signal from the detector D is amplified (>) and recorded (R).	20
1-6	Types of mass spectrometer analyzers: a) magnetic (m_i and z_i represent mass and charge, respectively), b) time-of-flight, c) quadrupole.	23
1-7	Block diagram of equipment for observation of Raman spectra.	24
1-8	Three most common types of arrangement of an optical sensor, where R is the reagent or selective layer, and S and D are the source and detector, respectively.	26
1-9	Gas-liquid chromatography via column separation: a) Mixture poured on top of column, b) partial separation, c) complete separation.	27
1-10	Spectrum of technologies in gas/liquid sensing.	30
2-1	Elution chromatography.	34
2-2	Typical chromatogram showing the output peaks for each subspecies.	36

2-3	Definition of retention time for output peak of length W	38
2-4	Definition of efficiency from Gaussian output peaks.	42
2-5	The effect of mobile phase flow rate on column efficiency.	44
2-6	Contribution of longitudinal diffusion and mass transfer terms to total efficiency.	48
2-7	Contrast between different resolutions for the same compounds A and B.	49
2-8	The general elution problem.	51
2-9	Typical components for a gas chromatography system: 1) Carrier gas supply; 2) Injection port; 3) Column; 4) Detector; 5) Gas supply for FID, (a) air, (b) hydrogen, (c) make-up gas.	52
2-10	Two of the first micro-chromatographs: From Terry, et al., 1979 [20] (left), and Manz, et al., 1987 [22](right).	54
3-1	Images showing the difference between $Nd : YAG$ (left), CO_2 (middle) and excimer laser (right) material processing results. Note the high degree of precision in the excimer case, and the absence of damage to the surrounding material (From Poulin et al, 1988 [35]).	57
3-2	Image showing of 5 μm diameter holes machined in a human hair using an excimer laser (From Poulin et al, 1988 [35]).	59
3-3	SEM photograph of an array of 70 μm square holes etched in 25 μm thick polyimide film. The webbing between the holes is 35 μm wide. The time taken to drill approximately one thousand such holes was one second (From Poulin et al, 1988 [35]).	60
3-4	Image showing an example of the removal of a polymer film from a metallic substrate (From Poulin et al, 1988 [35]).	61
3-5	Image showing an example of the removal of a thin metal film from a polymer substrate (From Poulin et al, 1988 [35]).	62
3-6	Image showing the difference between CO_2 (left) and excimer laser (right) marking of a glass material (From Poulin et al, 1988 [35]). . .	62

3-7	Pharmaceutical application.	63
4-1	Micro-column manufacturing setup.	65
4-2	Photograph showing micro-column manufacturing setup.	66
5-1	Excimer laser ablation sampling and analysis setup.	72
6-1	Photograph showing two quartz micro-columns.	77
6-2	Influence of excimer laser pulse frequency on component concentration for SaranWrap. Concentration of the three major components (A, B, C) of the ablation gases shown. Ablation time was 40 s and injection volume 0.3 ml.	80
6-3	Influence of injection volume on component concentration for SaranWrap. Ablation frequency of 100 Hz and ablation time of 40 s. . . .	80
6-4	Influence of ablation time on component concentration for SaranWrap. Ablation frequency of 100 Hz and injection volume of 0.3 ml. . . .	81
6-5	Influence of excimer laser pulse frequency on component concentration for polyethylene. Four major components (A, B, C, D) of ablation gases shown. Ablation time was 40 s and injection volume 0.3 ml. . .	81
6-6	Influence of injection volume on component concentration for polyethylene. Ablation frequency of 100 Hz and ablation time of 40 s. . . .	82
6-7	Influence of ablation time on component concentration for polyethylene. Ablation frequency of 100 Hz and injection volume of 0.3 ml. .	82
6-8	Results for pulse frequency variation experiments for SaranWrap. Clockwise starting from the top left corner: 10 Hz, 50 Hz, 75 Hz, and 100 Hz.	86
6-9	Results for injection volume variation experiments for SaranWrap. Clockwise starting from the top left corner: 0.1 ml, 0.2 ml, 0.4 ml, and 0.6 ml.	87

6-10	Results for ablation time variation experiments for SaranWrap. Clockwise starting from the top left corner: 60 seconds, 90 seconds, and 120 seconds.	88
6-11	Results for pulse frequency variation experiments for polyethylene. Clockwise starting from the top left corner: 10 <i>Hz</i> , 50 <i>Hz</i> , 75 <i>Hz</i> , and 100 <i>Hz</i>	89
6-12	Results for injection volume variation experiments for polyethylene. Clockwise starting from the top left corner: 0.1 <i>ml</i> , 0.2 <i>ml</i> , 0.4 <i>ml</i> , and 0.6 <i>ml</i>	90
6-13	Results for ablation time variation experiments for polyethylene. Clockwise starting from the top left corner: 60 seconds, 90 seconds, and 120 seconds.	91
A-1	Cell Drawing (Front Section).	96
A-2	Cell Drawing (Back Section).	97
A-3	Cell Drawing (Plexiglas Section).	97
A-4	Assembly Drawing.	98
B-1	Pulse Generator Circuit Diagram	99

List of Tables

2.1	Classification of chromatography.	35
2.2	Variables that affect column efficiency.	43
4.1	Properties of clear fused quartz (Adapted from Bolz et al, 1973 [44]).	69
D.1	File FID00095.D-Frequency rate of 10 <i>Hz</i> for SaranWrap.	103
D.2	File FID00096.D-Frequency rate of 50 <i>Hz</i> for SaranWrap.	103
D.3	File FID00097.D-Frequency rate of 75 <i>Hz</i> for SaranWrap.	103
D.4	File FID00098.D-Frequency rate of 100 <i>Hz</i> for SaranWrap.	104
D.5	File FID00099.D-Injection volume of 0.1 <i>ml</i> for SaranWrap.	104
D.6	File FID00100.D-Injection volume of 0.2 <i>ml</i> for SaranWrap.	104
D.7	File FID00101.D-Injection volume of 0.4 <i>ml</i> for SaranWrap.	104
D.8	File FID00102.D-Injection volume of 0.6 <i>ml</i> for SaranWrap.	104
D.9	File FID00103.D-Ablation time of 60 <i>s</i> for SaranWrap.	105
D.10	File FID00104.D-Ablation time of 90 <i>s</i> for SaranWrap.	105
D.11	File FID00105.D-Ablation time of 120 <i>s</i> for SaranWrap.	105
D.12	File FID00106.D-Frequency rate of 10 <i>Hz</i> for polyethylene.	105
D.13	File FID00107.D-Frequency rate of 50 <i>Hz</i> for polyethylene.	106
D.14	File FID00108.D-Frequency rate of 75 <i>Hz</i> for polyethylene.	106
D.15	File FID00109.D-Frequency rate of 100 <i>Hz</i> for polyethylene.	106
D.16	File FID00110.D-Injection volume of 0.1 <i>ml</i> for polyethylene.	106
D.17	File FID00111.D-Injection volume of 0.2 <i>ml</i> for polyethylene.	106
D.18	File FID00112.D-Injection volume of 0.4 <i>ml</i> for polyethylene.	107
D.19	File FID00113.D-Injection volume of 0.6 <i>ml</i> for polyethylene.	107

D.20 File FID00114.D-Ablation time of 60 s for polyethylene.	107
D.21 File FID00115.D-Ablation time of 90 s for polyethylene.	107
D.22 File FID00116.D-Ablation time of 120 s for polyethylene.	107

Chapter 1

Introduction

The sampling and analysis of chemicals has been an area of wide research and development for many decades now. The advent of miniaturization technology has greatly increased the potential for smaller, better performance, and versatile chemical sampling and analysis devices. One of the projects which is developing such technology is the Total Home Automation and Eldercare Systems Consortium which has the objective to take a lead in the development of fundamental technologies for home automation and home-based eldercare systems. As part of the research consortium, one of the projects is to design and construct a device which can analyze chemical gases and liquids (see Figure 1-1). The idea is to be able to introduce a fluid via a pump into the device, to detect and analyze the fluid by any one of several methods (e.g., chromatography, spectroscopy), which might include the addition of agents to the fluid as sample pretreatment, and then to act accordingly after dispensing the fluid. The information gathered is to be communicated to a central computer via wireless communication for monitoring and diagnostic purposes. This device could be used as a multi-purpose sensor for the home. For instance, it may be used for carbon monoxide monitoring, stale or decayed food detection, smoke detection, and medical diagnosis. In order to make the device as non-invasive as possible, the possibility of using miniaturization technology is being investigated. Miniaturization will allow for a self-contained system with minimum interaction with the environment. In addition, miniaturization will make it more attractive to the consumer and minimize

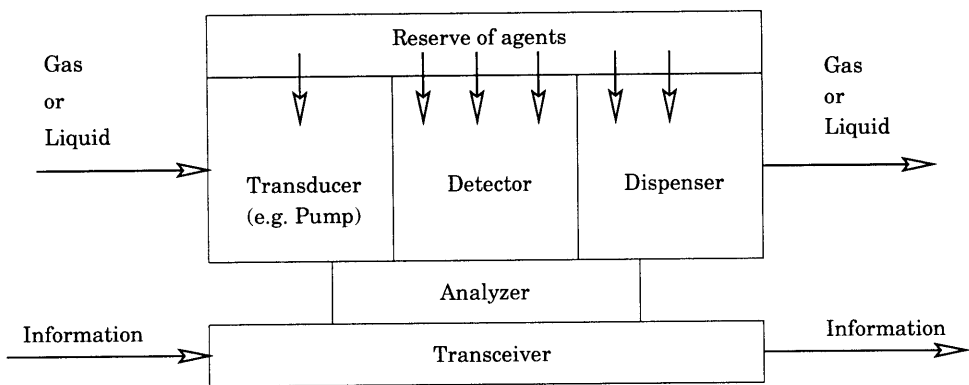


Figure 1-1: Block diagram for gas/liquid microanalyzer.

interference with any other tasks which may be necessary.

The project presents several challenges. These include the development of sensors and actuators for sampling and analyzing gases and liquids. Furthermore, there must be adequate communication between the sensors, actuators and information processing equipment to allow for proper operation of the device. The use of miniaturization technologies amplifies these challenges since the miniaturization process changes the overall physics of the system. The following paragraphs describe the motivation behind the microanalyzer project in more detail, and a summary of each of the different techniques of chemical gas and liquid detection being considered is given.

1.1 Overview of Chemical Analysis Technology

There exists a wide variety of chemical gas and liquid sensing and analysis technologies. These range from the cheaper, smaller, commercially-available smoke detectors for the home to the more sophisticated methods used in analytical chemistry such as spectroscopy and chromatography. Other general types of sensors include thermal, mass, electrochemical, and optical sensors. The following sections give a brief overview of each of these sensing technologies.

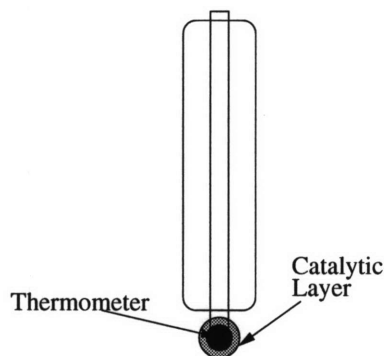


Figure 1-2: General schematic of a thermal catalytic sensor.

1.1.1 Thermal Sensors

Thermal sensors are based on the heat generated by a specific reaction as the source of analytical information [1]. The general strategy is to place a chemically selective layer on top of a thermal probe and to measure the heat evolved in the specific chemical reaction taking place in that layer, either as the change in temperature of the sensing element or as the heat flux through the sensing element (see Figure 1-2). The heat is evolved continuously, so thermal sensors are in a non-equilibrium state and their signal is obtained from a steady-state situation. An example of a thermal sensor is the enzyme thermistor, in which an enzyme-containing layer is deposited over a thermal probe and the substrate is allowed to diffuse into this from the sample solution which then reacts and the heat equal to the enthalpy of that reaction is evolved. Another example is that of the pyroelectric sensor. This sensor usually consists of a pyroelectric crystal which experiences a change in surface charge when it is heated [1]. A chemically selective material is usually applied to an electrode to generate heat when it reacts with another chemical. This heat of reaction causes the pyroelectric material to undergo a change in surface charge which can be measured. The major drawback of thermal sensors is the inherent tradeoff in their design. In order for the sensor to interact with the chemical analytes, it must exchange matter which means that it must be a thermodynamically open system. On the other hand, in order to obtain a maximum response it should be as adiabatic, or thermally insulated, as possible. In other words, ideal conditions for proper operation are difficult to attain

which limits the sensors' performance.

1.1.2 Mass Sensors

Mass sensors use the change of mass which occurs during the interaction of chemical species and the sensing element as their principle of operation [1]. Piezoelectric materials have found wide use in mass sensor development due to their small size, high sensitivity, and stability. Another example of a mass sensor is the surface acoustic wave sensor (SAW). These devices are based on the propagation of surface acoustic waves along solid surfaces in contact with a medium of low density. Thus when addition of mass during sensing using one of these devices takes place, a change in the magnitude of the amplitude of wave propagation, frequency shift, or phase shift can be measured and expressed as a function of concentration. A surface acoustic wave sensor usually consists of a transmission or delay line in which an acoustic wave is piezoelectrically generated in one oscillator, propagated along the surface of the substrate, and then transformed back to an electrical signal in the receiving oscillator (Figure 1-3). Analytical information is then obtained from the interaction of the sample with the propagating wave in the region of the transmission line. Selective chemical layers may also be used to enhance selectivity in these devices.

The major advantages of mass sensors are their simplicity of construction and operation, their light weight, and the low power consumption [1]. Compared to electrochemical sensors the measurement is carried out in a monopolar mode, i.e., only a single physical probe is necessary. Mass sensors have a high sensitivity and can be used for a very broad range of compounds. A major drawback is a high vulnerability to interferences. Also, the sensor will operate properly only if the interaction between species and the sensor results in a net change of mass of the chemically selective layer attached to the crystal being used. Mass sensors are also limited when used in liquid phases. In this case the output signal of the sensor is not only affected by the incremental mass due to the reaction, but also by frictional effects at the sensor-liquid interface that affect the energy loss [1].

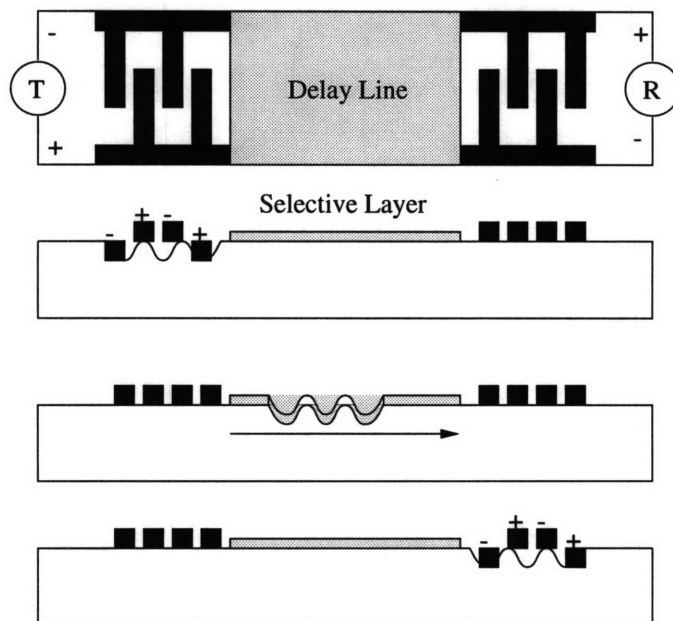


Figure 1-3: Schematic of a SAW sensor with transmitter T, receiver R, and the chemically selective layer deposited on the delay line.

1.1.3 Electrochemical Sensors

Electrochemical sensors are the largest and oldest group of chemical sensors [1]. Many members of this group have reached commercial maturity while many are still in various stages of development. Electrochemical sensors are divided by their mode of measurement into potentiometric (measurement of voltage), amperometric (measurement of current), and conductimetric (measurement of conductivity) sensors. They include enzyme electrodes, high-temperature oxide sensors, fuel cells, and surface conductivity sensors. The name electrochemical is due to the fact that there is a transfer of charge from an electrode to another phase, which may be a solid or liquid sample. In this process chemical changes occur at the electrodes and the charge is conducted through the bulk of the sample phase. Both the electrode reactions and/or the charge transport can be modulated chemically and serve as the basis of the sensing process [1].

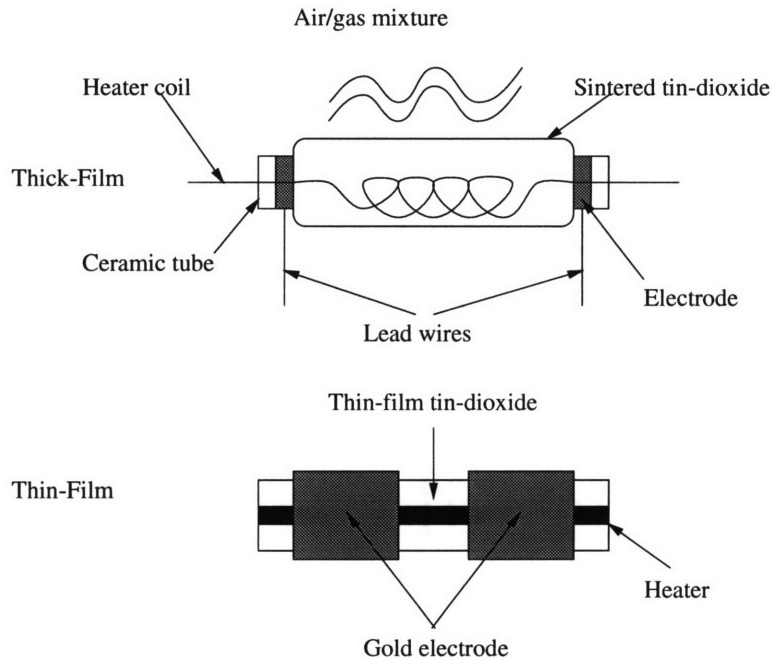


Figure 1-4: Operation of the tin-oxide sensor.

The Tin-Oxide Sensor

The most commonly used commercially-available electrochemical sensor is the tin-oxide sensor which has a high sensitivity to a wide range of gases. Some of the companies involved in this area include Figaro, Nimoto, Matsushita Panasonic, and Texas Instruments [2]. There are two types of tin-oxide sensors available in the market: thin and thick-film. The main advantage of the thin-film version is its smaller size (Figaro design is 3 to 1) and a lower power consumption. They both operate in the same manner: Gas molecules react with chemisorbed oxygen species on the sensor which results in a change in the conductivity (see Figure 1-4). These sensors operate at an elevated temperature ($100\text{-}600^{\circ}\text{C}$) which is provided by a heater. The heater provides two functions: it speeds up the reaction rate and it helps avoid water absorption onto the surface of the sensor. Tin-oxide sensors are quite sensitive to combustible materials ($0.1\text{-}100\text{ ppm}$) such as alcohols, but are generally poor at detecting sulfur- or nitrogen-based gases [2]. Catalytic metals may be incorporated within the sintered tin-oxide to control the selectivity of the sensor.

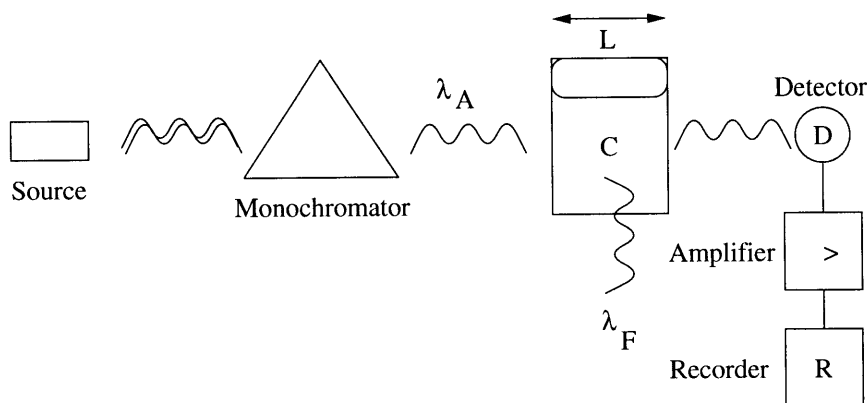


Figure 1-5: General arrangement of a spectroscopic absorption/emission experiment. Cuvette of a defined path length L contains solution of concentration C . The single wavelength radiation (λ_A) irradiates the sample and the attenuated radiation or secondary radiation (λ_F) are used to evaluate the extent of the interaction. The signal from the detector D is amplified ($>$) and recorded (R).

1.1.4 Optical Sensors

The interaction of electromagnetic radiation with matter takes place over a wide range of frequencies and usually in a highly specific manner. The study and use of these interactions comprise the domain of spectroscopy which provides information ranging from the electronic structure of atoms to the dynamics of polymeric chains [1]. In the most general conventional arrangement, the sample is irradiated with monochromatic radiation and the extent of the interaction is evaluated from the attenuation of the original radiation or by observing the secondary radiation emitted from the sample (Figure 1-5). The absorption of the primary radiation can also be coupled to other, non-optical effects, such as the increase in temperature or pressure, or the change in electrical conductivity.

Optical sensors and classical spectroscopic measurements use the same equipment, but the difference comes in the arrangement of the experiment itself [1]. In spectroscopic measurements the sample is generally placed in a well-defined path of the beam and the emerging radiation is captured by the detector. In the case of optical sensors, the beam is captured by the spectrophotometer, allowed to interact with the sample, and then reintroduced into the spectrophotometer in either its primary or secondary form for further processing. The need to guide and change the light over some dis-

tance limits the frequency range within which optical sensors can be used. The large spectroscopic knowledge base forms the basis for the development of optical sensors. The following sections describe some of the spectroscopic methods that have found wide use in chemical analysis as well as some examples of optical sensors.

Mass Spectroscopy

Mass spectroscopy refers to the destructive analytical method which can reveal specific characteristics about a compound's structure [3]. The technique is used mostly in a qualitative manner. The most important searched-for ion in the mass spectrum is the molecular ion because it directly indicates the molecular weight of the compound. During ionization, a considerable amount of excess energy can be transferred to the molecular ion, which, depending on its stability, may decompose into many fragment ions. These ions define subsets of atoms which may be related to functional groups or structural components of the original molecule. The set of fragment ions, which are represented by peaks in a mass spectrum, is often called a fragmentation pattern. Usually, the indication of molecular weight is sufficient enough to indicate the presence of a compound. However, it is better to compare the major peaks in the experimental results with those in a reference mass spectrum of the compound being sought. If molecular structure is of importance, careful study of the fragmentation pattern is crucial. Fragmentation of the compound-of-interest is efficiently achieved by electron ionization (EI) or chemical ionization (CI) which is a more "gentle" ionization technique that leaves more appreciable populations of molecular ions. Chemical ionization does not provide good information about structure though since the molecular ions that result from CI are relatively stable and they tend not to fragment into ions which could help in determining the identity and arrangement of functional groups in the molecule. For this reason, EI and CI are usually used in a complementary way to obtain reliable results.

Another consideration is the purity of the sample-of-interest. One must ensure that the sample being analyzed is as pure as possible [3]. In order to do this, a gas chromatography-mass spectrometer combination is often necessary to separate the

compound-of-interest from others.

Three of the common basic types of mass spectrometers are the magnetic, time-of-flight, and quadrupole (see Figure 1-6). Each of them have their own advantages and disadvantages.

The magnetic mass spectrometer (Figure 1-6a) is composed of a wedge-shaped magnetic field which disperses the total, unresolved ion beam from the ion source into discrete ion beams of individual mass per unit charge values by a process of direct focusing [1]. The ions which leave the ion source are accelerated in the mass spectrometer as they pass a potential which imparts kinetic energy to the ions. If an ion enters the magnetic field (which is perpendicular to the line of flight of the ion), it will be subjected to a magnetic force. This results in the ion following a circular path determined by balancing of the magnetic force by the centripetal force. From Figure 1-6a, it can be observed that when ions enter the magnetic field they follow circular paths of different radii (which depend on the different mass-to-charge ratios $\frac{m}{z}$) and only one of these will be of the correct value for an ion to reach the detector.

Time-of-flight mass spectrometers (Figure 1-6b) operate by measuring the time necessary for an ion to travel from the ion source to the detector [1]. All of the ions receive the same kinetic energy during acceleration but since they have different masses, they separate into groups according to velocity (and, hence, mass) as they traverse the region between the ion source and detector in the flight tube.

Finally, quadrupole mass spectrometers use a combination of DC and radio frequency (RF) potentials as a mass filter [1]. The quadrupole analyzer consists of four parallel electrodes with hyperbolic, elliptical, or circular cross-section (Figure 1-6c). The diagonally opposite electrodes (arranged symmetrically with the minimum-radius curve innermost) are at the same potential and are separated by a distance equal to twice the minimum radius of curvature. A potential is applied to the electrode to accelerate the ions. Once inside the rods, ions can have stable or unstable trajectories depending on the initial position and direction of movement of the ion when it enters the quadrupole. Once stability is established, stable ions are filtered and detected after passage through the quadrupole. Mass scanning is done by varying the voltage

applied to the electrodes.

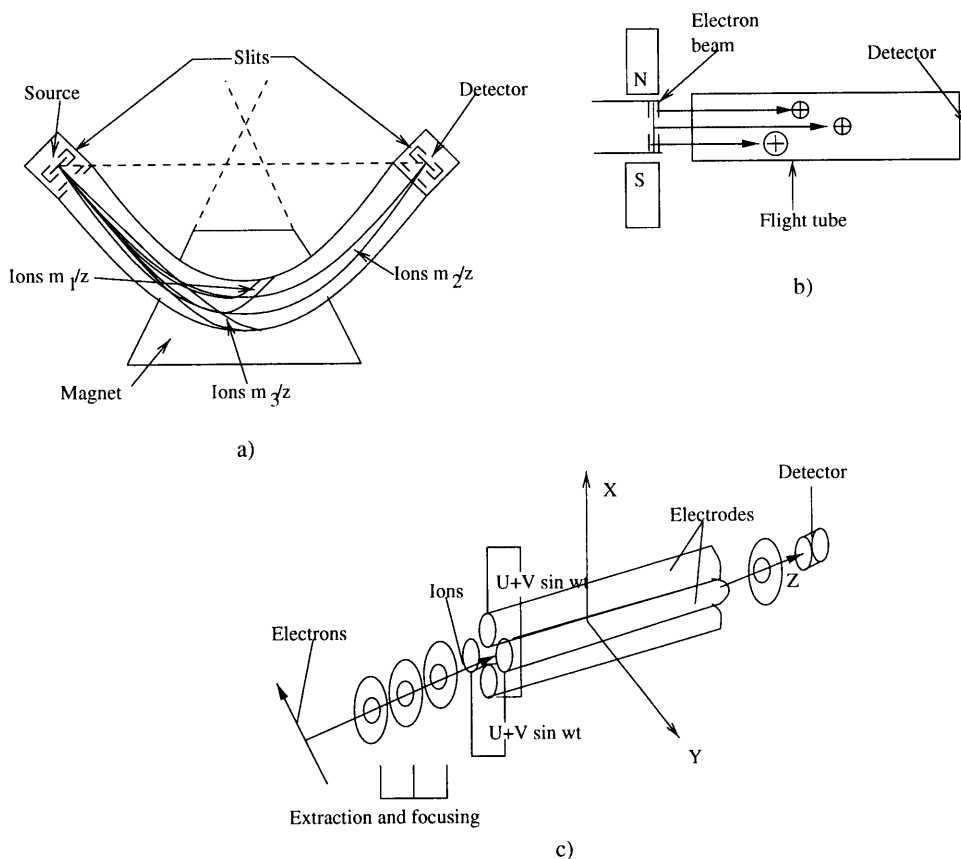


Figure 1-6: Types of mass spectrometer analyzers: a) magnetic (m_i and z_i represent mass and charge, respectively), b) time-of-flight, c) quadrupole.

Raman Spectroscopy

Raman spectroscopy refers to the phenomenon of scattering when monochromatic radiation is incident on gases, liquids or solids [4]. If the frequency content of the scattered radiation is analyzed, the results show not only the frequency of the incident light but also, in general, pairs of new frequencies. These frequencies are found to lie primarily in the ranges associated with transitions between rotational, vibrational, and electronic levels of the fluid's molecules. The scattered radiation usually has polarization characteristics which are different from that of the incident light, and both the intensity and polarization of the scattered radiation depend on the direction of observation. The scattering is usually now made using a suitable laser and detected

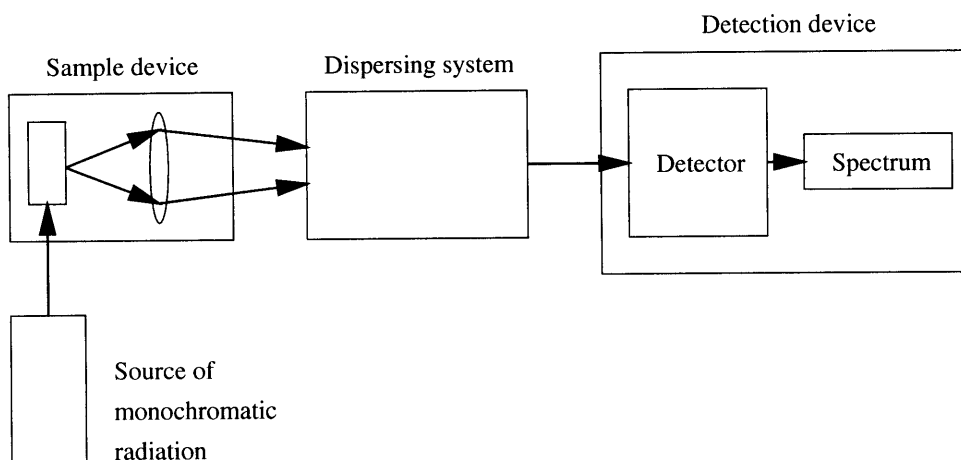


Figure 1-7: Block diagram of equipment for observation of Raman spectra.

photoelectrically. Figure 1-7 shows the block diagram of the equipment needed for observation of Raman spectra. The source of monochromatic radiation is usually a laser. The sample device is where the sample to be considered is illuminated and its scattered radiation collected using some kind of lens configuration. The dispersing system usually consists of a diffraction grating. Finally, the detection device consists of a photographic plate in the case of a spectrograph, or a special kind of photocell in the case of a spectrometer.

Problems with Raman include fluorescence and thermal sample degradation [4]. The high sensitivity of Raman spectroscopy can be drastically reduced when weak scattering occurs in the presence of background fluorescence, a situation often encountered. Thermal decomposition of samples under intense focused laser beam is also encountered. These two problems can be avoided by using Fourier Transform Raman (FT-Raman) spectroscopy. Since both problems are related to absorption of the incident photons by some species in the sample, the way to avoid them is to use an incident laser frequency that avoids all absorption processes. FT-Raman uses this idea and other additional instrumentation to bypass the problems of fluorescence and thermal sample degradation [5].

There are several advantages to using Raman spectroscopy over other techniques such as infrared (IR) spectroscopy [4]. Since Raman scattering from molecular vibrations can be measured in the visible region of the spectrum, the optics of the

instrument are relatively simple. Sensitive detectors with high signal-to-noise ratios are available. The intrinsic weakness of the Raman effect necessitates the use of an intense monochromatic light source, and, as such, the laser is ideal. A decided advantage of Raman spectroscopy is that a wide part of the spectrum is obtained with the same instrument and cell, giving more information in a shorter time. Infrared is applicable to almost any kind of sample but some materials (intractable polymers, single crystals, and aqueous solutions) are quite difficult to handle. With Raman spectroscopy, sample preparation is remarkably simple and the capability for using glass or quartz cells is a marked advantage (they are both transparent to Raman). Its principal limitation is with high colored or fluorescing materials.

Miniaturization of the spectroscopic methods just described has been an area of study for some years now [6]. Miniaturization of some of the subcomponents are possible. In terms of sources of laser radiation, optical fibers can be a possible tool. The detectors can be composed of miniature diode arrays. Furthermore, diffraction gratings may be made using deep-etch X-ray lithography, which is the first step of the LIGA manufacturing technique [6]. One of the major limitations in terms of miniaturization is the optical path length needed for some of the spectrometers which limits the physical size and performance of the spectrometer.

Some Optical Sensors

The principle source of selectivity in optical sensors, like in any other type of sensor, is provided by a chemically selective layer through the specific interactions with the chemical to be determined. This selective layer can be placed on the optical fiber in several different ways, depending on the type of interaction used. The simplest arrangement for absorption studies uses two fibers facing each other across a gap, which is filled with the selective layer [1]. One fiber delivers and the other collects the light with some acceptable efficiency (Figure 1-8a). The gap dimensions define the optical path length required for proper operation. Another configuration is the use of two parallel fibers and a mirror, which reflects the light into the collection fiber. The detection limit is improved since the light traverses the selective layer

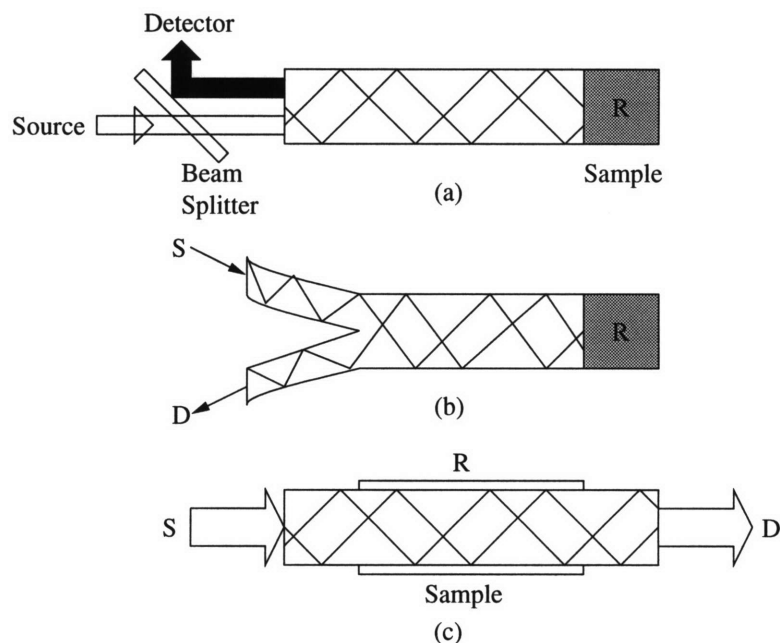


Figure 1-8: Three most common types of arrangement of an optical sensor, where R is the reagent or selective layer, and S and D are the source and detector, respectively.

twice. A similar arrangement uses only one bifurcated layer, which transmits both the initial and final intensity (Figure 1-8b). The simplification at the sensing end leads to complications at the instrumentation end, where the two beams must be separated by mirrors, beam splitters, and other necessary hardware, and piped to the appropriate parts of the spectrophotometer. The reflecting surface in these two implementations can be a mirror or a scattering surface. In any case the sensor has the appearance of a monolithic probe. Optical sensors based on absorption, fluorescence, phosphorescence, and luminescence can employ these two configurations.

The second possibility is to make use of the continuous evanescent field which exists at the surface of an optical fiber and place the selective layer within this field (Figure 1-8c). For such an arrangement the protective coating and cladding are replaced by the selective layer in a short segment of the fiber [1].

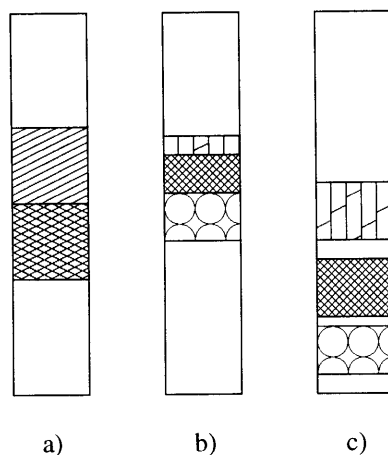


Figure 1-9: Gas-liquid chromatography via column separation: a) Mixture poured on top of column, b) partial separation, c) complete separation.

1.2 Gas-Liquid Chromatography

Gas-Liquid Chromatography (GLC) refers to a technique of separating substances [7]. This method relies on the relative movement of two phases with one of them being fixed (stationary phase) and the other one moving (mobile phase). A column is usually used to separate a mixture (see Figure 1-9). The column is packed with porous material coated with a layer of liquid, usually water. The stationary phase is the liquid layer and the solid merely serves as a support for it. A small sample of the mixture is introduced into the column which then forms a band of absorbed material. When the solvent is allowed to flow through the column it carries with it the components of the mixture. The rate of movement of a given component depends on its solubility in the stationary phase. Hence, more soluble substances travel more slowly through the column than the less soluble ones. During their travel the substances undergo partition between the two phases and separation takes place because of the difference in the partition coefficients. All separations by chromatography depend on the fact that the substances which are being separated distribute themselves between the mobile and stationary phases in proportions which vary from one substance to another.

1.3 Applications for Chemical Analyzers

There are countless of applications for gas and liquid sensors and analyzers. These range from smoke detectors to process control sensors for food and beverage processing. The following sections describe these and other applications in more detail.

1.3.1 Home

The number one concern in the home, as far as gas sensors are concerned, is the establishment of clean air and the maintaining of clean air [2]. There are several gases of importance for gas sensing in the home. These include carbon monoxide, carbon dioxide, methane, propane, radon, and smoke. These gases can be poisonous when high enough concentrations are present (carbon monoxide/dioxide), they can cause respiratory problems (radon), or they may indicate dangerous situations (smoke, methane, and propane). Other possible applications for the home include air quality detectors, ethanol sensors in microwaves to improve cooking quality, sensors for combustion control in heaters and furnaces, and food spoilage or freshness sensors for the refrigerator or kitchen area.

1.3.2 Healthcare

In the healthcare area, chemical sensors can be very useful for diagnostic purposes. Examples of these include acetone detection in the breath for the diagnosis of diabetes, and the detection of oxygen content in the blood which is used to diagnose several medical conditions. Other applications include sensors for low levels of certain drugs in urine, and monitoring of glucose levels in diabetic patients to control insulin injections [8].

1.3.3 Environmental

Aside from healthcare and the home, chemical sensors have several other potential applications. The drive to improve combustion efficiency and reduce pollutant gas

products is very strong. The Environmental Protection Agency has requirements of smokestack monitoring of such combustion products as nitrous oxides, sulfur oxides and carbon monoxide which usually require exotic detection techniques (e.g., infrared absorption techniques) which are currently very costly. The competitive advantage of cheaper, smaller sensor technologies is obvious in this case [8].

1.3.4 Automotive and Defense

In the automotive area, sensors may be useful for climate control (e.g., humidity sensors), oil change indication, and exhaust pollution monitoring (e.g., nitrous and sulfur oxides, carbon monoxide). In the defense field, one of the most commonly-mentioned applications for chemical sensors is that of a portable low-level nerve gas monitor. As chemical and biological weapons become more of a threat, such a tool can help prevent prolonged exposure to dangerous levels of chemical and biological species [8].

1.3.5 Other Applications for Chemical Sensors

In the biotechnology area sensors for process yield and fermentation progress can be very useful [8]. These may include sensors for dissolved oxygen, carbon monoxide, sodium, potassium, chloride, calcium, pH, and sensors for various sugars and metal ions. Two more fields where chemical sensors may be useful are wastewater treatment and food and beverage processing. Monitoring and controlling the waste levels in discharged process water is a very attractive application for chemical sensors. Among the most important species to be monitored are hydrocarbons in general, and process solvents in particular, as well as heavy-metal ions, dissolved ammonia, chlorine and pesticides. Chemical sensors in the food and beverage processing area include sensors for continuous pH monitoring during various processing steps, and sensors for sulfur dioxide, which is used as a preservative in many foods and in beverages such as wine, where a minimum useful concentration is important to maintain proper flavor and aroma. Chemical sensors for monitoring the fermentation of wines, beer

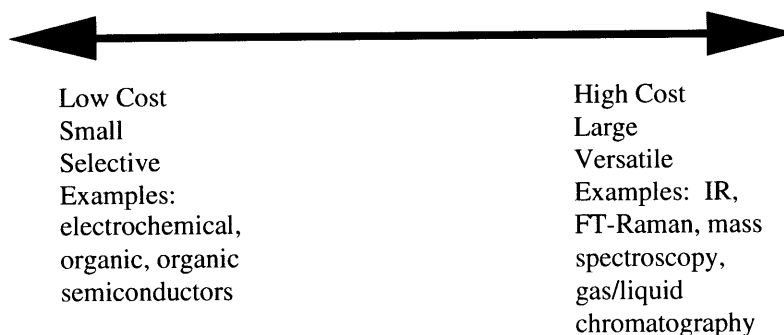


Figure 1-10: Spectrum of technologies in gas/liquid sensing.

and alcohol would improve uniformity and reduce costs. Devices for this purpose would include sensors for glucose, fructose, ethyl alcohol, pH, dissolved oxygen, dissolved carbon dioxide, malic acid and tartaric acid. Other general purpose sensors may include potassium-ion sensors, sodium sensors, chloride sensors and calcium sensors. Although many of the latter chemical sensors exist in one form or another, they currently are not very useful in the food processing business because of surface contamination problems and high maintenance requirements.

1.4 Motivation for Micro-analyzer Development

As described in the previous sections, there are several technologies for gas and liquid analysis for a wide range of needs. These technologies can be separated into two broad categories (see Figure 1-10). At the lower end of the technology spectrum we have small, low cost, selective sensing technologies such as electrochemical and organic sensors. These include commercially-available sensors for the home such as carbon monoxide and smoke detectors. At the other end of the spectrum we have the high cost, larger, yet more versatile methods for gas sensing and analysis, such as spectroscopic methods (infrared, FT-Raman), and chromatography (gas, liquid). The following sections describe the general problems with the lower end sensing technologies and thus provide motivation for the use of higher-end technologies for the microanalyzer project.

1.4.1 Lower-End Sensor Technology Problems

The problems with current lower-end sensor technology include limited selectivity, baseline drift, calibration, nonlinearity in the response of the sensor, size, high power consumption and operating temperature, and sensor poisoning. In terms of selectivity, no sensor is specific enough, i.e., a sensor will be sensitive to other gases, humidity, and temperature [2]. Second, sensor baseline drift with time is usually caused by several environmental factors such as temperature and humidity. In addition, calibration and training of sensors must be portable to other nominally identical sensors especially if the sensor baseline drifts over time. Also, sensor response is nonlinear for current sensors which adds complexity to the problem. Most current commercially-available sensor technology is relatively large compared to miniaturized devices, and operation is at high temperatures which means a high power consumption (e.g., tin-oxide sensor). Reactant gases also tend to poison sensors over time which affects the sensor reliability.

Some of the methods that may be used to overcome the problems just discussed can be in terms of design. For example, selectivity may be enhanced by having an array of non-selective (wide-band) sensors with broadly overlapping sensitivities. This is known as the electronic nose approach [9, 10, 11, 12]. The use of temperature and pressure modulation may also be used to improve selectivity. In terms of signal processing, the use of pre- and post-filtering of the signals (e.g., averaging, pattern recognition techniques), may be useful to compensate for drift, nonlinearity, and other environmental factors [9, 10, 11, 13]. Fourier analysis and sensor signal deconvolution using Gaussian functions have also been found to be useful tools for compensation and selectivity purposes [14, 15, 16, 17]. Even though these techniques for sensor improvement exist, there are still several practical problems in terms of long-term reliability and robustness which have not been solved and which have limited the operation of lower-end sensors.

There is a definite technological advantage in using the higher-end sensing and analysis technologies on the right of the technology spectrum shown in Figure 1-10,

and for this reason the decision was made to concentrate on utilizing these in the microanalyzer project. In order to minimize the higher cost and larger size of this technology, the miniaturization of such a device is being investigated. By doing this there will be several benefits. First, the small size of the microanalyzer will make it an attractive tool for on-site monitoring such as in environmental, industrial and combat settings. Second, with time its small size should help reduce the cost of such a system once production becomes cost effective. Thirdly, by concentrating on higher-end technologies, the system will have the versatility that other sensors don't have in terms of the variety of compounds which can be analyzed, increased sensitivity and robustness against drift and other factors. Another important advantage of using higher end technologies is their long history and the vast amount of knowledge base which exists as a result of it. The techniques that have been developed over the years can be very useful in optimizing a miniaturized system.

In particular, miniaturization of gas chromatographic systems has several benefits. First, aside from the portability and lower power consumption which miniaturization brings, smaller column diameters help improve column efficiencies, and the lower volumes help reduce cost in terms of mobile phase and stationary phase amounts required. An introduction to gas chromatography and a brief history of miniaturization in chromatography will be described in the next chapter.

1.4.2 Thesis Overview

The following two chapters will describe the two topics of focus in this thesis, that is, gas chromatography and excimer laser ablation. These chapters are followed by chapters which describe the quartz micro-column manufacturing process which was developed, and the excimer laser ablation products sampling and analysis technique which was studied. Experimental setup and results are presented and discussed, and finally, suggestions for future work are made.

Chapter 2

Gas Chromatography

Chromatography offers a way to separate and characterize complex mixtures of liquids or gases. In this section the basic theory behind gas chromatography is described and a brief history of the development of micro-chromatographs for the characterization of complex gas and liquid mixtures is introduced.

2.1 Introduction

Chromatography is an analytical method that is widely used for the separation, identification, and determination of the chemical components in complex mixtures, many of which could not otherwise be resolved [18]. In general, chromatography uses a stationary phase and mobile phase which can be either a gas or a liquid. Components of a mixture are carried through the stationary phase by the flow of the gaseous or liquid mobile phase. Separations are based on the differences in migration rates among the sample components. Figure 2-1 shows a schematic which explains how chromatography works in general. A single portion of the sample dissolved in the mobile phase is introduced at the head of the column, whereupon components A and B distribute themselves between the two phases. Introduction of additional mobile phase (the eluent) forces the dissolved portion of the sample down the column, where further partition between the mobile phase and fresh portions of the stationary phase takes place. Partitioning between the fresh solvent and the stationary phase takes

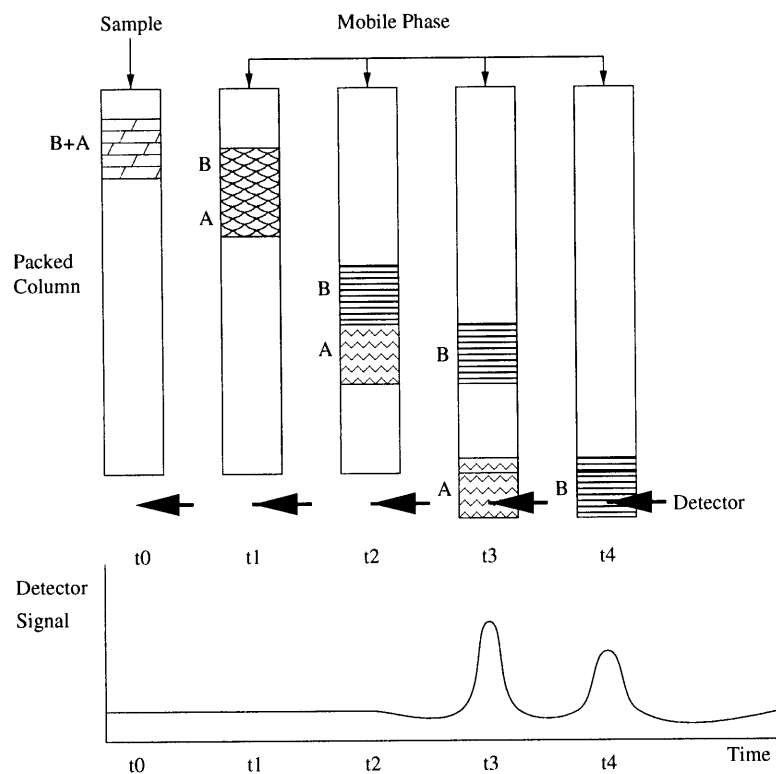


Figure 2-1: Elution chromatography.

place simultaneously at the site of the original sample. Further additions of solvent carry solute molecules down the column in a continuous series of transfers between the two phases. Since solute movement can occur only in the mobile phase, the average rate at which a solute migrates depends upon the fraction of time it spends in that phase. This fraction is small for solutes that are strongly retained by the stationary phase (B), and large where retention in the mobile phase is more likely (A). Ideally, the resulting differences in rates cause the components in a mixture to separate into bands, or zones, along the length of the column. Isolation of the separated species is then accomplished by passing a sufficient quantity of mobile phase through the column to cause the individual bands to pass out at the end (to be eluted from the column), where they can be collected.

General	Specific	Stationary Phase	Equilibrium
Liquid Chromatography (Mobile phase-liquid)	Liquid-liquid or partition	Liquid adsorbed on a solid	Partition between immiscible liquid
	Liquid-bonded phase	Organic species bonded to a solid surface	Partition/adsorption
	Liquid-solid, or adsorption	Solid	Adsorption
	Ion exchange Size exclusion	Ion-exchange resin Liquid in interstices of a polymeric solid	Ion-exchange Partition/sieving
Gas Chromatography (Mobile phase-gas)	Gas-liquid Gas-bonded phase	Liquid adsorbed on a solid Organic species bonded to a solid surface	Partition between gas and liquid Partition/adsorption
	Gas-solid	Solid	Adsorption

Table 2.1: Classification of chromatography.

2.1.1 Classification of Chromatography

Classification of chromatographic methods is based on either the physical means by which stationary and mobile phases are brought into contact with each other (e.g., column and planar chromatography), or by whether the mobile phase is a liquid or a gas (e.g., liquid, gas chromatography) [18]. Each type varies according to the specific method that is used to bring the mobile and stationary phases into contact, the stationary phase used, and the type of equilibrium which takes place during the separation process. Table 2.1 summarizes the different types of chromatography generally encountered in the field.

2.1.2 Chromatograms

The performance of any chromatographic separation is based on the output from the detector at the end of the column. This is usually in the form of a chromatogram.

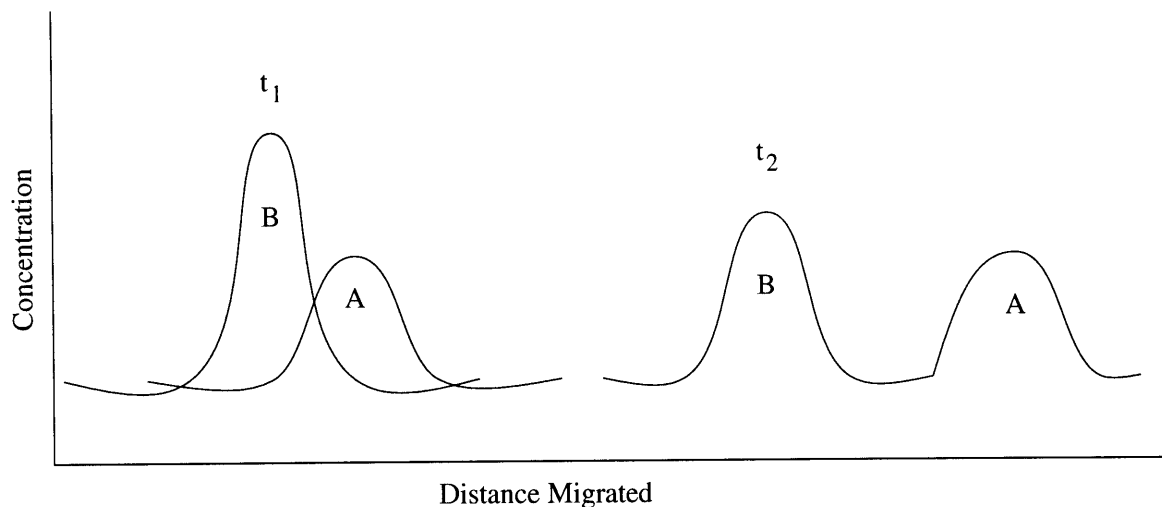


Figure 2-2: Typical chromatogram showing the output peaks for each subspecies.

A chromatogram is a plot showing the solute concentration detected at the end of the column versus time (or volume of added mobile phase) [18]. The positions of the peaks on the time axis can be used to identify the components of the sample, while the areas under the peaks provide a quantitative measure of the amount of each species. Figure 2-2 shows a typical chromatogram which shows the output of a detector. The chromatogram shows that species B is more strongly retained by the stationary phase than A. The distance between the two increases as they move down the column. The time from the point of sample introduction into the column to the time the peaks appear in the chromatogram is known as the retention time for that particular peak. In Figure 2-2 t_1 and t_2 correspond to the retention times for compounds A and B, respectively.

2.2 Migration Rates of Solutes

There exist several indices used to characterize chromatographic separations. These serve as a tool to describe the physical variables involved in the separation process as well as to provide a way to measure the performance of the separations, find optimal values for each separation, and to have some way of comparing different chromatographic separations in terms of efficiency. The following sections discuss these in

greater detail.

2.2.1 Partition Ratios

All chromatographic separations are based upon differences in the extent to which solutes are partitioned between the mobile and stationary phase [18]. The equilibrium constant for this reaction is called the partition ratio and it is defined as

$$K = \frac{c_S}{c_M} \quad (2.1)$$

where c_S is the molar analytical concentration of a solute in the stationary phase and c_M is its analytical concentration in the mobile phase. Ideally K is constant over a wide range of solute concentrations, that is, c_S is proportional to c_M . This condition is the basic assumption made when doing chromatography and in this case the process is referred to as linear chromatography.

2.2.2 Retention Times

As mentioned before, the retention time t_R is the time required for an output peak to reach the detector at the end of the column (see Figure 2-3) [18]. The peak at retention time t_M is for a species that is not retained by the column; its rate of migration is the same as the rate of motion of the molecules of the mobile phase. The retention time serves as the main indicator of compound presence in a mixture. It is used to differentiate between compounds once proper calibration with known standards has been carried out. The average linear rate of solute migration \bar{v} is

$$\bar{v} = \frac{L}{t_R} \quad (2.2)$$

where L is the length of the column packing. Similarly, the average linear rate of movement u of the molecules of the mobile phase is

$$u = \frac{L}{t_M} \quad (2.3)$$

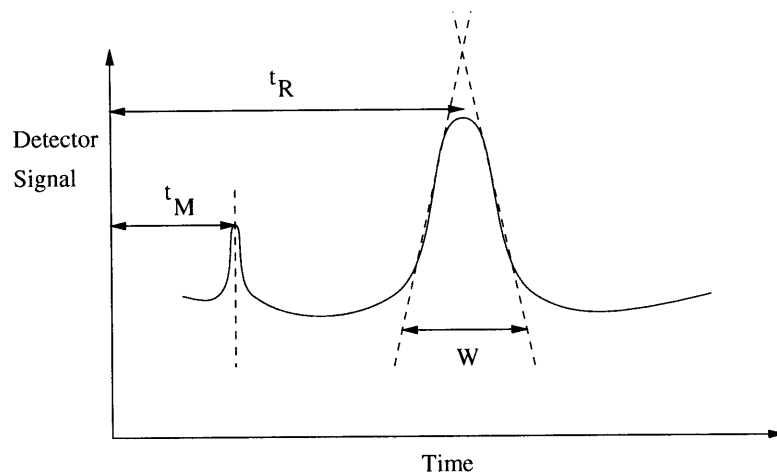


Figure 2-3: Definition of retention time for output peak of length W .

2.2.3 The Retention Time and Partition Ratio Relationship

In order to relate the retention time of a solute to its partition ratio, the migration rate is expressed as a fraction of the velocity of the mobile phase:

$$\bar{v} = u \times \text{fraction of time solute spends in mobile phase} \quad (2.4)$$

This fraction is equal to the average number of moles of solute in the mobile phase at any instant divided by the total number of moles of solute in the column [18]:

$$\bar{v} = u \times \frac{\text{moles of solute in mobile phase}}{\text{total moles of solute}} \quad (2.5)$$

$$\bar{v} = u \times \frac{c_M V_M}{c_M V_M + c_S V_S} = u \times \frac{1}{1 + \frac{c_S V_S}{c_M V_M}} \quad (2.6)$$

where c_M and c_S are the molar concentrations of the solute in the mobile and stationary phases, respectively, and V_M and V_S are the total volumes of the two phases in the column. After some manipulation using Equation 2.1 and Equation 2.6, an expression for the rate of solute migration as a function of its partition ratio and the

volumes of the stationary and mobile phases is obtained:

$$\bar{v} = u \times \frac{1}{1 + K \frac{V_S}{V_M}} \quad (2.7)$$

The two volumes may be estimated from the method by which the column is prepared [18].

2.2.4 The Rate of Migration of Solutes: The Capacity Factor

The capacity factor is an important parameter that is widely used to describe the migration rates of solutes in columns [18]. For a solute A, the capacity factor is defined as

$$k'_A = K_A \frac{V_S}{V_M} \quad (2.8)$$

where K_A is the partition ratio for the species A. Substitution of Equation 2.8 into Equation 2.7 yields

$$\bar{v} = u \times \frac{1}{1 + k'_A} \quad (2.9)$$

After some manipulation of Equation 2.9 using Equations 2.2 and 2.3, it can be shown that the capacity factor can be obtained from a chromatogram:

$$k'_A = \frac{t_R - t_M}{t_M} \quad (2.10)$$

When the capacity factor for a solute is much less than unity, elution goes on so rapidly that accurate determination of the retention times is difficult. When the capacity factor is larger than perhaps 20 to 30, elution times become inordinately long. Ideally, separations are performed under conditions in which the capacity factors for the solutes in a mixture lie in the range between 1 to 5. Capacity factors can be varied by changing temperature and column packing. In liquid chromatography, capacity factors can often be manipulated to give better separations by varying the composition of the mobile phase and the stationary phase [18].

2.2.5 Differential Migration Rates: Selectivity Factor

The selectivity factor of a column for the two species A and B is defined as

$$\alpha = \frac{K_B}{K_A} \quad (2.11)$$

where K_B is the partition ratio for the more strongly retained species B and K_A is the constant for the less strongly held or more rapidly eluted species A. By this definition, α is always greater than unity. Substituting Equation 2.8 into Equation 2.11 yields

$$\alpha = \frac{k'_B}{k'_A} \quad (2.12)$$

which relates the selectivity factor for two solutes and their capacity factors where k'_B and k'_A are the capacity factors for B and A, respectively. Substitution of Equation 2.10 for the two solutes into Equation 2.12 gives

$$\alpha = \frac{(t_R)_B - t_M}{(t_R)_A - t_M} \quad (2.13)$$

which shows that the selectivity factor can be determined from an experimental chromatogram. The selectivity factor is useful in describing differential migration rates between two compounds being separated [18].

2.3 Band Shapes and Band Broadening

Theory of column chromatography must address the following phenomena:

1. Differential migration rates of solutes.
2. The Gaussian shapes of chromatographic peaks.
3. Peak broadening.

The previous section addressed differential migration rates and in this section the shapes and breadths of chromatographic peaks are considered.

2.3.1 The Shapes of Chromatographic Peaks

The rate or kinetic theory of chromatography describes the shapes of peaks in quantitative terms based on a random-walk mechanism for the migration of molecules through a column [18]. Peaks' shapes are similar to Gaussian curves which can be attributed to the additive combination of the random motions of the myriad solute particles as the chromatographic band moves down the column. The result of these random individual processes is a symmetric spread of velocities around the mean value, which represents the behavior of the average particle. The breadth of the band increases as it moves down the column because more time is allowed for spreading to occur. Thus, zone breadth is directly related to residence time in the column and inversely related to the flow velocity of the mobile phase.

2.3.2 Efficiency of Chromatographic Columns

There are two widely used parameters as measures of the efficiency of chromatographic columns [18]:

1. Number of theoretical plates N .
2. Plate height H (or, sometimes, height equivalent of a theoretical plate HETP).

The two are related by $N = \frac{L}{H}$ where L is the length of the column packing. Efficiency increases as the number of plates becomes greater and as the plate height becomes smaller. Efficiencies can vary from a few hundred to several hundred thousand (in terms of plate numbers). Plate heights from a few tenths to one thousandth of a centimeter or smaller are not uncommon.

2.3.3 The Plate Height and Band Broadening Relationship

Since chromatographic bands are Gaussian and because efficiency of a column is reflected in the breadth of chromatographic peaks, it is convenient to define H in

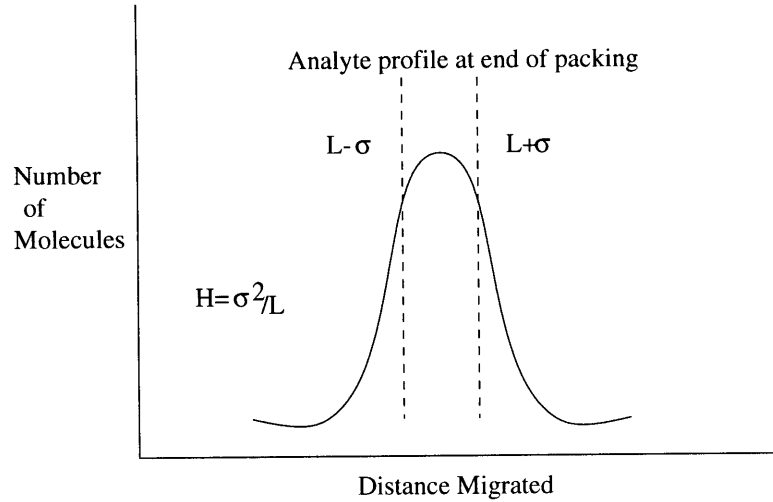


Figure 2-4: Definition of efficiency from Gaussian output peaks.

terms of variance per unit length of column:

$$H = \frac{\sigma^2}{L} \quad (2.14)$$

where H is the plate height. This is also illustrated in Figure 2-4. The plate height can be thought of as the length of column that contains a fraction of the analyte that lies between L and L minus the variance. Because the total area under the normal error curve bounded by plus or minus sigma is about 68 % of the total area, the plate height, as defined, contains 34 % of the analyte [18].

2.3.4 Experimental Evaluation of N and H

Variance of peak in terms of time is given by

$$\tau = \frac{\sigma}{\left(\frac{L}{t_R}\right)} \quad (2.15)$$

where $\frac{L}{t_R}$ is the average linear velocity of the solute. It can be shown that

$$N = 16 \left[\frac{t_R}{W} \right]^2 \quad (2.16)$$

Variable	Symbol	Units
Linear velocity of mobile phase	u	m/s
Diffusion coefficient in mobile phase	D_M	m^2/s
Diffusion coefficient in stationary phase	D_S	m^2/s
Capacity factor	k'	unitless
Diameter of packing particle	D_p	m
Thickness of liquid coating on stationary phase	D_f	m

Table 2.2: Variables that affect column efficiency.

Thus N can be calculated from measurements of the retention time and the peak width W which is 4 times the variance of the peak. To obtain H , L must be known. Another method used to approximate N , believed to be more reliable, is to take one-half of the peak width W [18]. The number of theoretical plates is then given by

$$N = 5.54 \left[\frac{t_R}{W_{\frac{1}{2}}} \right]^2 \quad (2.17)$$

The two parameters N and H are widely used in the literature and by instrument manufacturers as measures of column performance. For these parameters to be meaningful in comparing two columns, it is essential that they be determined with the same compound [18].

2.4 Variables That Affect Column Efficiency

Band broadening is the consequence of the finite rate at which several mass-transfer processes occur during migration of a solute down a column [18]. Some of these rates are controllable by the adjustment of experimental variables, thus permitting improvement of separations. Table 2.2 lists the variables that affect column efficiency. The following sections describe some of these variables and their effects.

2.4.1 The Effect of Mobile-Phase Flow Rate

The magnitude of kinetic effects on column efficiency clearly depends upon the length of time the mobile phase is in contact with the stationary phase, which in turn depends upon the flow rate of the mobile phase. Efficiency studies have been made

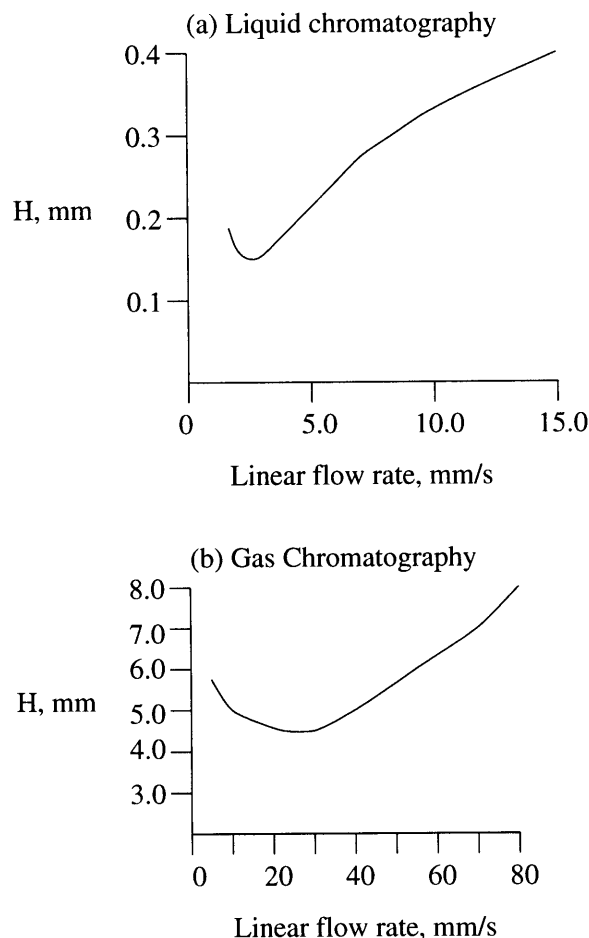


Figure 2-5: The effect of mobile phase flow rate on column efficiency.

to determine H as a function of mobile-phase velocity (Figure 2-5) [18]. Both plots in Figure 2-5 show a minimum in H (or maximum in efficiency) at low flow rates; the minimum for liquid chromatography (LC) usually occurs at flow rates that are well below those for gas chromatography (GC) and often so low that they are not observed under normal operating conditions. Generally, LC's are obtained at lower flow rates than GC's. Furthermore, plate heights for LC columns are an order of magnitude or more smaller than those encountered with GC columns. Offsetting this advantage

is the fact that it's impractical to employ liquid columns that are longer than about 0.25 to 0.5 m (because of high pressure drops), whereas GC columns may be 50 m or more in length. Consequently, the total number of plates, and thus overall column efficiency, are usually superior with GC columns.

2.4.2 A Theory of Band Broadening

There exist several theories which attempt to explain chromatographic band broadening. None of these is entirely adequate to explain the complex physical interactions and effects that lead to zone broadening and thus lower column efficiencies. Some of these have been useful though in pointing the way toward improved column performance. One of these is presented in the following paragraphs. It is based on the work carried out in the 1950's by Dutch chemical engineers and which led them to the van Deemter equation on which Equation 2.18 is based [18].

The efficiency of most chromatographic columns can be approximated by the expression

$$H = \frac{B}{u} + C_S u + C_M u \quad (2.18)$$

where H is the plate height, u is the linear velocity of the mobile phase, B is the longitudinal diffusion coefficient, while C_S and C_M are mass transfer coefficients for the stationary and mobile phases, respectively. The following sections describe each of these terms in greater detail.

The Longitudinal Diffusion Term $\frac{B}{u}$

Diffusion is a process in which species migrate from a more concentrated part of a medium to a more dilute one. The rate of migration is proportional to the concentration difference between the regions as well as to the diffusion coefficient D_M of the species. The latter, which is a measure of the mobility of a substance in a given medium, is a constant equal to the velocity of migration under a unit concentration gradient.

In chromatography, the longitudinal diffusion results in the migration of a solute

from the concentrated center of a band to the more dilute regions on either side (that is, toward and opposed to the direction of flow) [18]. Longitudinal diffusion is a common source of band broadening in GC but is of little significance in LC because the rate at which molecules diffuse in a gaseous medium is high, whereas the rate in a liquid solvent is relatively low. The magnitude of the longitudinal diffusion coefficient B is largely determined by the diffusion coefficient D_M of the analyte in the mobile phase and is directly proportional to this constant.

The contribution of the longitudinal diffusion to plate height is inversely proportional to the linear velocity of the eluent. Such a relationship is not surprising, since as the analyte is in the column for a briefer period when the flow rate is high, then diffusion from the center of the band to the two edges has less time to occur. The initial decrease in H shown in Figure 2-5 is a direct consequence of the longitudinal diffusion. Note that the effect is much less pronounced in LC because of the much lower diffusion rates in a liquid mobile phase. The striking difference in plate heights shown by the two graphs can also be explained by considering the relative rates of the longitudinal diffusion in the two mobile phases: diffusion coefficients in gaseous media are orders of magnitude larger than in liquids. Thus, band broadening goes on to a much greater extent in GC than in LC.

The Mass-Transfer Coefficients C_S and C_M

The need for the two mass transfer coefficients arises because the equilibrium between the mobile and the stationary phases is established so slowly that a chromatographic column always operates under non-equilibrium conditions [18]. Band broadening from mass-transfer effects arises because the many flowing streams of a mobile phase within a column and the layer of immobilized liquid making up the stationary phase both have finite widths. Consequently, time is required for the solute molecules to diffuse from the interior of these phases to their interface where transfer occurs. This time lag results in the persistence of non-equilibrium conditions along the length of the column. If the rates of mass transfer within the two phases were infinite, broadening of this type would not occur.

Note that the extent of both longitudinal broadening and mass-transfer broadening depend upon the rate of diffusion of the analyte molecules but that the direction of diffusion in the two cases is different. Longitudinal broadening arises from the tendency of molecules to move in directions that tend to parallel the flow, whereas mass-transfer broadening occurs from diffusion that tends to be at right angles to the flow. As a consequence, the extent of longitudinal broadening is inversely related to flow rate. For mass-transfer broadening, in contrast, the faster the mobile phase moves, the less time there is for equilibrium to be approached. Thus, the mass-transfer effect on plate height is directly proportional to the rate u of movement of the mobile phase. When the stationary phase is an immobilized liquid, the mass-transfer coefficient is directly proportional to the square of the thickness of the film on the support particles and inversely proportional to the diffusion coefficient D_S of the solute in the film. These effects can be understood by realizing that both reduce the average frequency at which analyte molecules reach the interface where transfer to the mobile phase can occur. That is, with thick films, molecules must on the average travel farther to reach the surface, and with smaller diffusion coefficients, they travel slower. The consequence is a slower rate of mass transfer and an increase in plate height [18].

When the stationary phase is a solid surface, the mass transfer coefficient C_S is directly proportional to the time required for a species to be absorbed or desorbed, which in turn is inversely proportional to the first order rate constant for the process [18].

The mobile-phase mass-transfer coefficient C_M is known to be inversely proportional to the diffusion coefficient of the analyte in the mobile phase D_M and also to be some function of the square of the particle diameter of the packing, the square of the column diameter, and the flow rate. The contributions of mobile-phase mass-transfer to plate height is the product of C_M (which is a function of solvent velocity) and the velocity of the solvent.

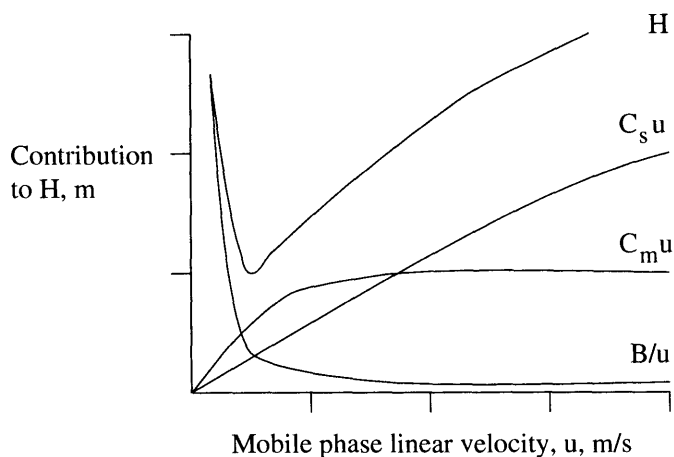


Figure 2-6: Contribution of longitudinal diffusion and mass transfer terms to total efficiency.

Contribution of Terms to Efficiency

Figure 2-6 shows the contributions of the longitudinal diffusion term and the mass-transfer terms to the total efficiency [18]. The longitudinal diffusion term is inversely proportional to flow rate of the mobile phase, while the mass-transfer terms are directly proportional to the flow as shown. The top curve is a summation of these various effects. Note that an optimum flow rate exists at which the plate height is a minimum and the separation efficiency is a maximum.

Summary of Methods for Reducing Band Broadening

There are several ways by which band broadening may be reduced [18]. Varying the diameter of the packing particles is one way to reduce band broadening since the mass-transfer coefficient of the mobile phase is a function of it. Also, reducing the diameter of the column can accomplish the task since the mass-transfer coefficient of the mobile phase C_M is proportional to the square of the column diameter. In the case of gas chromatography, varying the temperature can help reduce band broadening. This is because longitudinal diffusion can be reduced by lowering temperature (which means that the diffusion coefficient D_M is reduced as well). Finally, for liquid chromatography minimization of the thickness of the layer of absorbed liquid can help since C_S is proportional to the square of this variable.

2.5 Column Resolution

The resolution R_s of a column provides a quantitative measure of its ability to separate two analytes [18]. The resolution is defined as

$$R_s = \frac{2\Delta Z}{W_A + W_B} = \frac{2[(t_R)_B - (t_R)_A]}{W_A + W_B} \quad (2.19)$$

The resolution for a given stationary phase can be improved by lengthening the column, thus increasing the number of plates. An adverse consequence of the added plates, however, is an increase in the time required for the resolution. Figure 2-7

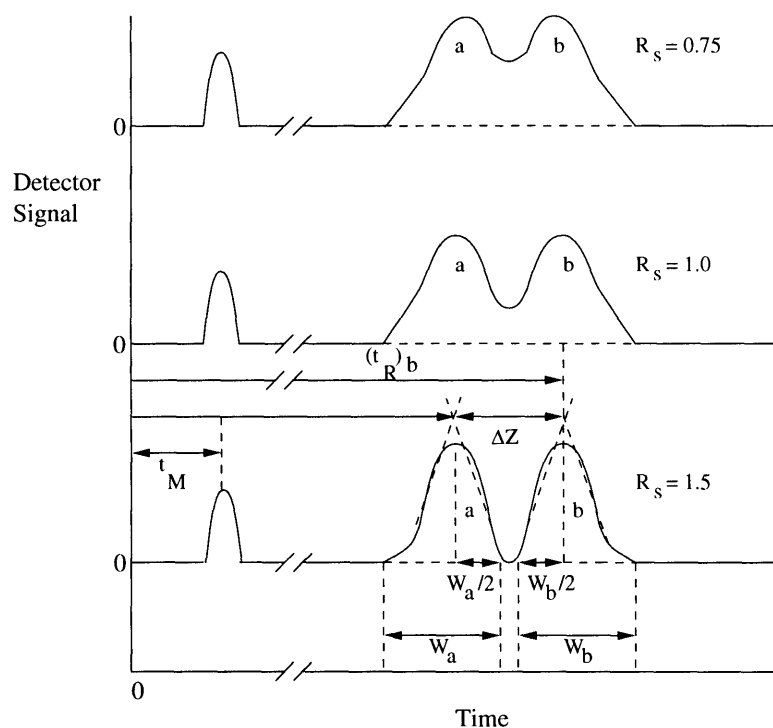


Figure 2-7: Contrast between different resolutions for the same compounds A and B.

illustrates the significance of the resolution. The figure consists of chromatograms for species A and B on three columns with different resolving powers.

2.5.1 The Relationship Between Resolution and Properties of the Column and Solute

A useful equation that relates the resolution of a column to the number of plates it contains as well as to the capacity and selectivity factors of a pair of solutes A and B on the column is given by

$$R_s = \frac{\sqrt{N}}{4} \left(\frac{\alpha - 1}{\alpha} \right) \left(\frac{k'_B}{1 + k'_B} \right) \quad (2.20)$$

where k'_B is the capacity factor of the slower-moving species and α is the selectivity factor [18]. This equation can be rearranged to give the number of plates needed to realize a given resolution:

$$N = 16R_s^2 \left(\frac{\alpha}{\alpha - 1} \right)^2 \left(\frac{1 + k'_B}{k'_B} \right)^2 \quad (2.21)$$

2.5.2 The Relationship Between Resolution and Elution Time

The goal of chromatography is to get the highest possible resolution in the shortest possible elapsed time. A compromise between the two is usually necessary [18]. The time required to elute two species with a resolution R_s is given by

$$(t_R)_B = \frac{16R_s^2 H}{u} \left(\frac{\alpha}{\alpha - 1} \right)^2 \frac{(1 + k'_B)^3}{k_B'^2} \quad (2.22)$$

where u is the linear rate of movement of the mobile phase.

2.5.3 Optimization Techniques

There exist several methods to optimize column resolution [18]. Variation of the plate height can be achieved by the variation of the particle size of the packing, reduction of the diameter of the column, variation of the column temperature (GC), and variation of the thickness of the liquid film (LC). Variation in the capacity factor can be achieved by temperature changes (GC), and changes in solvent composition

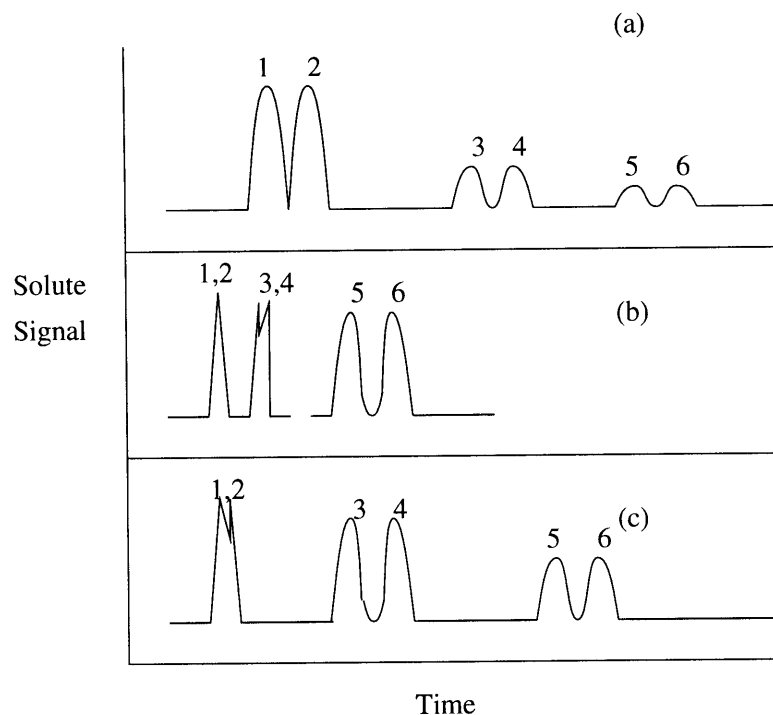


Figure 2-8: The general elution problem.

(LC). Variation in the selectivity factor can be achieved by changing the composition of the mobile phase, changing the column temperature, changing the composition of the stationary phase, and using special chemical effects.

2.6 The General Elution Problem

Figure 2-8 shows hypothetical chromatograms for a six-component mixture made up of three pairs of components with widely different distribution coefficients and thus widely different capacity factors. In chromatogram (a), conditions have been adjusted so that the capacity factors for components 1 and 2 are in the optimal range of 1 to 5. The factors for the other two components are far larger than the optimum, however. Thus, the peaks for components 5 and 6 appear only after an inordinate length of time has passed; furthermore, these peaks are so broad that they may be difficult to identify unambiguously. As shown in chromatogram (b), changing conditions to optimize the separation of components 5 and 6 bunches the peaks for the first four components to the point where their resolution is unsatisfactory. Here, however,

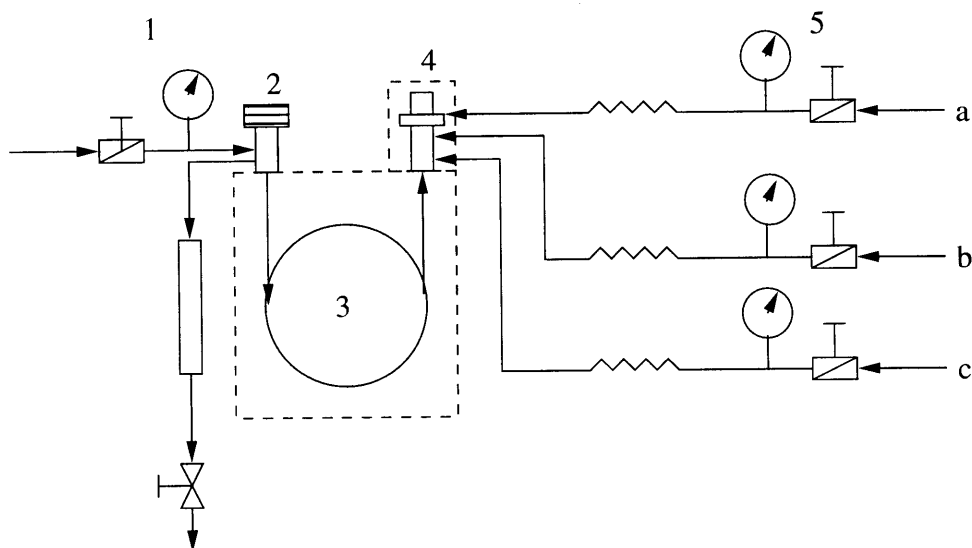


Figure 2-9: Typical components for a gas chromatography system: 1) Carrier gas supply; 2) Injection port; 3) Column; 4) Detector; 5) Gas supply for FID, (a) air, (b) hydrogen, (c) make-up gas.

the total elution time is ideal. A third set of conditions, in which the capacity factors for components 3 and 4 are optimal, results in chromatogram (c). Again, separation of the other two pairs is not entirely satisfactory.

The phenomenon illustrated in Figure 2-8 is encountered often enough to be given a name: the general elution problem [18]. It represents the general problem which must be solved in order to obtain good chromatographic results. A common solution to this problem is to change conditions that determine the values of the capacity factor k' as the separation proceeds. These changes can be performed in a stepwise manner or continuously (e.g., solvent programming (LC) and temperature programming (GC)).

2.7 Components of a Chromatography System

A typical gas chromatography system consists of a carrier-gas supply, a sample-injection system, a column, column thermostating system, a detector, and a liquid phase in the case of gas-liquid chromatography [19]. Figure 2-9 shows these components.

The carrier-gas supply usually consists of a chemically inert gas such as helium, argon, nitrogen, and hydrogen, to prevent the mixture to be separated from reacting with the mobile phase. The sample-injection system usually consists of a calibrated microsyringe. Columns usually consist of packed or open tubular columns. Column thermostating is usually accomplished using a thermostated oven. There exist a good variety of detectors. These include thermal conductivity, flame ionization, electron-capture, and selective detectors. The choice is usually determined by the desired response time, type of compounds to be separated, ruggedness and other desired characteristics. Liquid-phases for gas-liquid chromatography are chosen depending on the compound to be separated since some liquid phases work better with particular types of compounds but not so well with others.

2.8 Applications of Chromatography

2.8.1 Qualitative

The most popular qualitative application of chromatography is that of determining the presence or absence of components in a mixture that contains a limited number of possible species whose identities are known. Otherwise, the application of the technique is limited since the only information obtained from a chromatogram are the retention time and area for each peak [18].

2.8.2 Quantitative

Chromatography can be used for quantitative analysis by comparison of either the height or area of the analyte peak with that of one or more standards. If conditions are properly controlled, both of these parameters vary linearly with concentration [18].

Chromatography can serve as a first step in a qualitative analysis by various spectroscopic techniques. The combination of gas chromatographic and spectroscopic techniques is often found to enhance the characterization of complex mixtures [18].

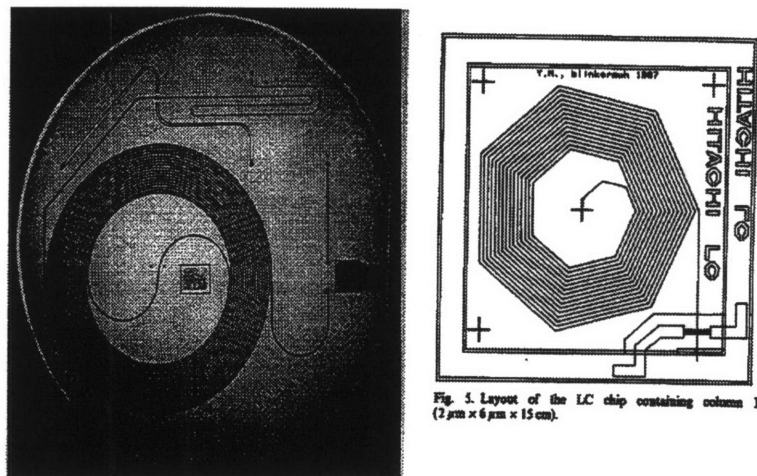


Figure 2-10: Two of the first micro-chromatographs: From Terry, et al., 1979 [20] (left), and Manz, et al., 1987 [22](right).

2.9 Micro-Chromatographs

There has been some work done in the area of micro-chromatography. The first known micro-gas chromatographic air analyzer is the one manufactured by Terry et al., 1979 (see Figure 2-10) [20, 21]. The miniature GC was fabricated using photolithography and chemical etching techniques and it consists of a sample injection valve and a 1.5 m long separating capillary column which were fabricated on a substrate silicon wafer (0.05 m diameter). The output thermal conductivity detector was separately batch fabricated and integrably mounted on the substrate wafer. The performance of the device showed separations in less than 10 seconds with a number of theoretical plates ranging from 385 to 2300 plates (compared to 10k-100k for very long and efficient standard capillary columns).

Following this work it wasn't until 1987 that Manz et al. [22], developed a miniature open-tubular column liquid chromatograph (see Figure 2-10). The device consisted of a silicon chip with an open-tubular column, a conductimetric detector, a chip holder and a pressure pulse driven injector using a conventional liquid chromatography pump and valves. The chip and open-tubular column had dimensions of 5 mm × 5 mm and 6 μm × 2 μm × 0.15 m, respectively. The performance showed efficiencies of 8000 to 25000 plates in 1 and 5 minutes, respectively. The total column volume

was 1.5 nanoliter and the detection cell volume was 1.2 picoliter.

Other results in this research area include the development of an electrochemical flow cell (20 *nl*) integrated with an enzyme immobilized column [23], the automated repetitive sample injection and separation on a time scale of seconds [24, 25], fast separations (150 *ms*) for liquid phase analyses [26, 27, 28], continuous sample pre-treatment using a free-flow electrophoresis device integrated onto a silicon chip [29], and the development of a glass microchip with postcolumn reactor fabricated to conduct post separation derivatization [30].

Aside from the limitation on column efficiency for these two systems, the pressure drop requirements for the column were affected by the smaller diameter. Hence there was a limit to how small the column could be made. In order to overcome this problem, the use of an electric field for separation has been used (electrophoresis) more currently as an alternative to pressure-based flow since the electric-field strength is not affected by the smaller diameter of the column [31, 32, 33, 34]. Another problem is that the photolithography and chemical etching techniques used to make these micro-chromatographs produce rectangular cross-section columns which limits column performance due to likely turbulence caused by the sharp corners. Furthermore, for these two systems one of the column sides consisted of a glass cover which may not necessarily have prevented leakage of carrier gas and analytes.

As these two examples show, the technology for miniaturization of gas chromatography systems exists. The next steps are to improve the performance and reliability of such devices. This includes improvement in fabrication techniques, signal processing and component performance. Miniaturization of gas chromatographic systems has several benefits. First, aside from the portability and lower power consumption which miniaturization brings, a smaller column diameter helps improve column efficiencies, resolutions, speeds up separations as the previous sections described, and the resulting lower volumes help reduce cost in terms of mobile phase and stationary phase amounts required. To this end, the possibility of manufacturing actual tubular microcolumns using quartz tubing has been investigated as part of this thesis. This work is described in Chapter 4.

Chapter 3

Excimer Laser Ablation

3.1 Introduction

Excimer laser ablation has been found to be an excellent tool for a wide range of applications. In particular, the use of excimer lasers for material processing has been found to provide excellent results in terms of extremely high precision and excellent edge definition; absence of any significant charring or burning of the surrounding material; minimal heat-affected zone; little, if any distortion of the bulk material; selective removal of material from the underlying substrate, leaving the substrate virtually unaffected; and definition of patterns by mask imaging rather than by translation of the focused spot [35]. The following sections describe the basic operation of the excimer laser, the excimer laser ablation process, the analysis of excimer laser ablation products, and some of the application areas in which excimer lasers have found use.

3.2 Excimer Lasers

Excimer lasers operate in high-pressure mixtures such as XeF_2 (xenon fluoride), $XeCl_2$ (xenon chloride), $KrCl_2$ (krypton chloride), KrF_2 (krypton fluoride), and ArF_2 (argon fluoride). The operation is based on the electron bombardment of the gas mixture which causes a series of reactions that lead to the formation of an excited complex such as XeF^* [36]. This excited complex is unstable in its ground state and

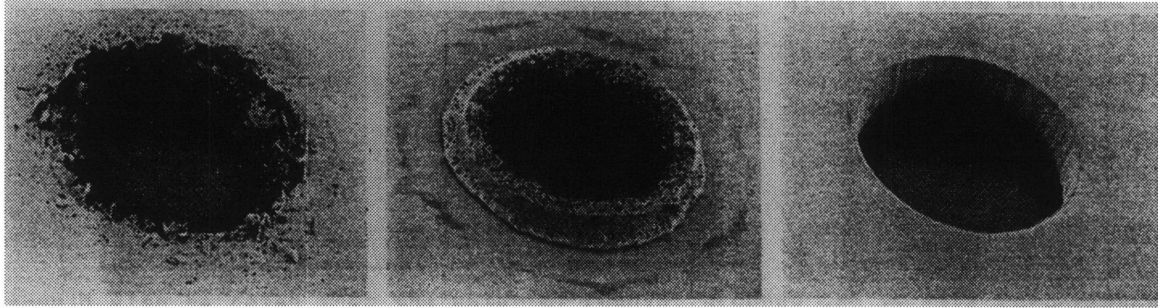


Figure 3-1: Images showing the difference between *Nd : YAG* (left), *CO₂* (middle) and excimer laser (right) material processing results. Note the high degree of precision in the excimer case, and the absence of damage to the surrounding material (From Poulin et al, 1988 [35]).

therefore dissociates immediately on emitting light. Commercially-available excimer lasers are sources of intense pulsed ultraviolet radiation. This radiation is not inherently of narrow linewidth since the laser transition occurs from a bound to a repulsive state of the excimer and is therefore not of well-defined energy. Excimer lasers are however good sources for pumping dye lasers. The development of new and existing excimer lasers is an active field and there have been major improvements in operating performance and reliability in recent years [36].

3.3 Excimer Laser Materials Processing

The main advantage of excimer lasers for materials processing applications is their ultraviolet (UV) output. In particular, it has been shown that the short pulses of UV radiation from excimer lasers are able to ablate organic material very cleanly, leaving well-defined edges and resulting in minimal damage to the surrounding unexposed material [35] (see Figure 3-1). The general physical mechanisms of excimer laser ablation are discussed next, followed by a discussion about the analysis of ablation products.

3.3.1 Physical Mechanisms of Ablation

Excimer laser ablation is governed by non-thermal mechanisms unlike those associated with *YAG* and *CO₂* laser processing. The simplified version of the physical mechanism of excimer laser ablation has been given by [37]. When UV radiation is incident on a sample of organic material, absorption takes place in a very thin layer near the surface, as most organic materials exhibit high absorption coefficients in the UV range. The absorbed photons are efficient at breaking the bonds found in organic compounds, and when the rate of bond breaking exceeds a critical value, also known as the fluence threshold, the material decomposes ablatively. The driving forces for this phenomenon are: (i) the large increase in the specific volume of the material's fragments compared to the polymer chains they replace, and (ii) the excess energy of the UV photon compared to the chemical bond that is broken. In this manner, the ablated material is removed layer by layer on a pulse by pulse basis. Typically, each pulse removes only a fraction of a micrometer of the polymer. The actual ablative mechanism has been found to be more complex than this, consisting of both photochemical and photothermal components. The relative contributions of thermal and photochemical processes for the ablation of material have been demonstrated using calorimetry and acoustic studies [38]. Regardless of what the precise mechanism is, there is no doubt that the edge quality produced by excimer laser cutting is better than can be obtained with thermal laser cutting processes as can be seen in Figure 3-2.

The material removal process can be very dependent on factors such as laser wavelength, energy fluence, and repetition rate. Generally, for any one material, different fluence thresholds for ablation are observed for the different excimer laser wavelengths, with the lowest threshold corresponding to the shortest wavelength. This is consistent with the higher photon energy and shallower absorption depth associated with the shorter wavelengths. For this reason, much of the early work on photoablative decomposition was carried out using the *ArF* excimer laser at 193 *nm* as this laser will produce the cleanest cuts in the broadest range of materials. However, for technical

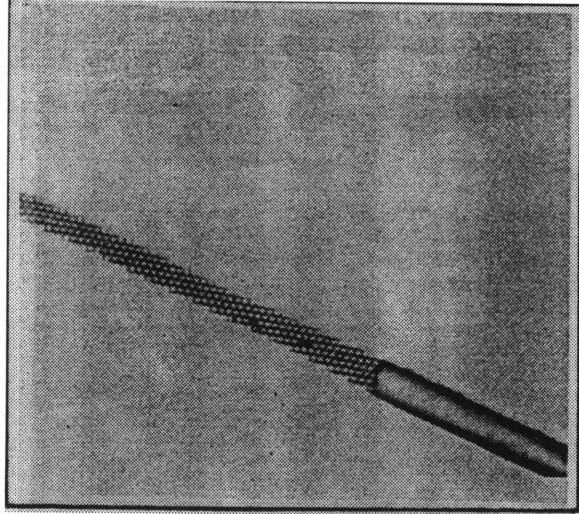


Figure 3-2: Image showing of $5\ \mu\text{m}$ diameter holes machined in a human hair using an excimer laser (From Poulin et al, 1988 [35]).

reasons, it is desirable to use either the *KrF* or *XeCl* excimer laser at $248\ \text{nm}$ and $308\ \text{nm}$, respectively. Fortunately, it has been demonstrated that a large number of materials can be processed at these longer wavelengths, thus providing a reasonable amount of flexibility in system design.

3.3.2 Excimer Laser Ablation Product Analysis

The analysis of excimer laser ablation products has been limited to the analysis of products for study of the excimer laser process rather than for material characterization purposes. Past efforts have included the use of excimer lasers for ablation of a variety of polymers including polyimide, polyetheretherketone, and polystyrene as well as arterial wall, atherosclerotic plaque, and cardiovascular tissue [39, 40, 41].

Specifically, studies of *XeCl* excimer ablation of polyetheretherketone, a high temperature thermoplastic, has been carried out [39]. Volatile products of ablation included carbon monoxide, acetylene, and small quantities of low molecular weight hydrocarbons. Other results include the ablation of arterial wall which yielded gaseous products in the form of methane, ethylene, and low molecular weight hydrocarbons [40], and the ablation of polyimide under the influence of the ambient atmosphere on the ablation products [41]. These are just a few of the many studies which have been

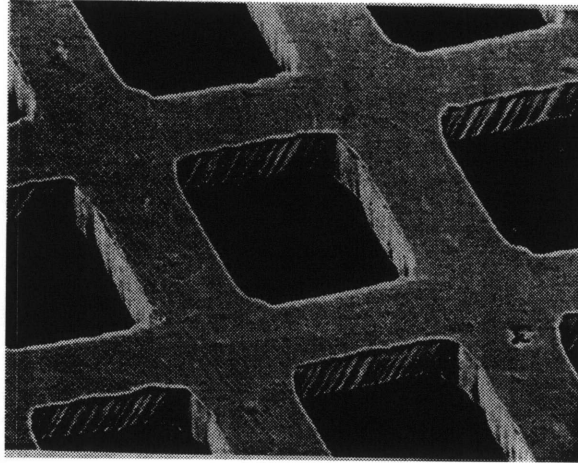


Figure 3-3: SEM photograph of an array of $70 \mu\text{m}$ square holes etched in $25 \mu\text{m}$ thick polyimide film. The webbing between the holes is $35 \mu\text{m}$ wide. The time taken to drill approximately one thousand such holes was one second (From Poulin et al, 1988 [35]).

carried out in the area of excimer laser ablation in the past two decades.

3.4 Application Areas

The most common applications for excimer laser ablation include machining of free standing polymers, removal of polymer films from metal substrates and vice versa, micromachining of ceramics and semiconductors, and marking of thermally sensitive materials [35].

In the area of machining free-standing polymer films, excimer laser ablation offers several advantages over the commonly-used CO_2 laser whose thermal cutting action limits the minimum size of hole which may be made as well as the density of the holes, particularly in thin samples. Excimer laser ablation virtually eliminates the heat-affected zone, and allows for precise drilling of small diameter holes in thin materials at spacings not much greater than the hole diameter. In addition, because of the unique features of the ablative process, a large number of holes can be drilled at one time using an appropriate masking technique (see Fig. 3-3).

There exists a wide difference in threshold fluences between organic materials ($10^6 \frac{\text{mJ}}{\text{m}^2}$) and thick metal films ($> 10^4 \frac{\text{J}}{\text{m}^2}$), and for this reason the removal of thin films

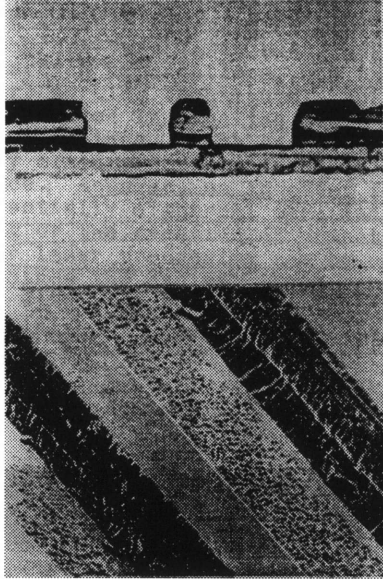


Figure 3-4: Image showing an example of the removal of a polymer film from a metallic substrate (From Poulin et al, 1988 [35]).

such as polymer films, adhesives, and photoresists from metallic substrates is a great application for excimer laser ablation. This includes relatively thin substrates, which would not tolerate the heat associated with conventional laser processing. Figure 3-4 shows a pair of $150\ \mu\text{m}$ wide slots machined into a $4\ \text{mm}$ polyimide-adhesive layer on a $2\ \text{mm}$ thick copper substrate. The boundary between the polyimide and adhesive layers remains clearly visible after processing, and the copper substrate is clean and undisturbed, ready for subsequent process steps. The reverse operation, that is, the removal of thin metal or semiconductor films from polymer or glass substrates is also an area of excimer laser ablation application. Figure 3-5 shows an SEM photograph of $75\ \mu\text{m}$ wide slots etched in a $0.2\ \mu\text{m}$ thick gold film on a $1\ \text{mm}$ polyester substrate. The lower trace shows the sample at increased magnification and shows the excellent edge quality that can be achieved by this process.

In the area of laser marking, excimer lasers provide removal of material with minimal thermal conduction to the surrounding material thus providing clean markings without micro-cracking or thermal stress introduction. Figure 3-6 shows the difference between CO_2 and excimer laser based marking of a glass material. The fine micro-cracking seen in the CO_2 case is not present at all in the excimer case.

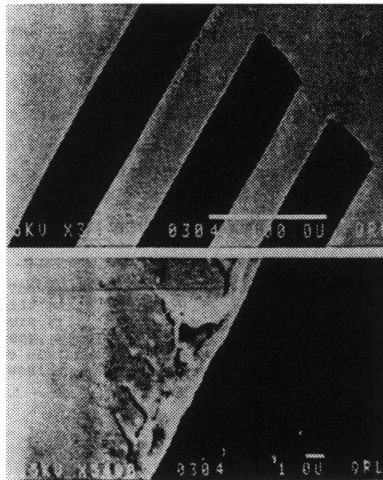


Figure 3-5: Image showing an example of the removal of a thin metal film from a polymer substrate (From Poulin et al, 1988 [35]).

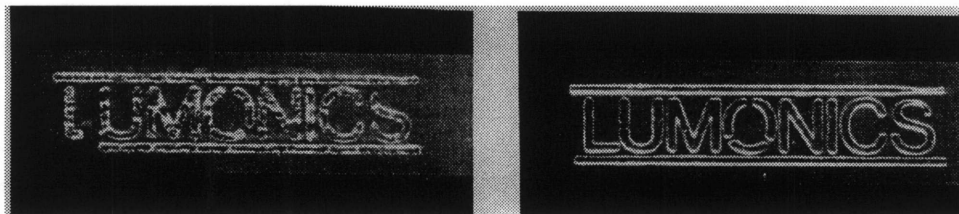


Figure 3-6: Image showing the difference between CO_2 (left) and excimer laser (right) marking of a glass material (From Poulin et al, 1988 [35]).

One of the applications being considered for this technology is in the pharmaceutical area. A major limitation for pharmaceutical companies is the long time it takes them to introduce new drugs. Usually this involves automation on a large scale using robotics and many new compounds which have to be analyzed. Determination of the usefulness of these compounds as potential drugs is done on a trial-and-error basis to a certain extent. Miniaturization of the process should help reduce time, increase the number of compounds which can be analyzed and in the long run, decrease the cost of development. A possible device suggested by Professor Ian W. Hunter is shown in Figure 3-7. A diamond plate is used to retain an array of compounds which is moved by a piezotube in the X-Y plane to reach any desired location. A Peltier-effect heat pump on the diamond plate can be used for thermal control. In addition, lasers can be used to scan the compounds for analysis and a micro-column may be used for “smelling” these compounds via a gas chromatographic system. Furthermore, the

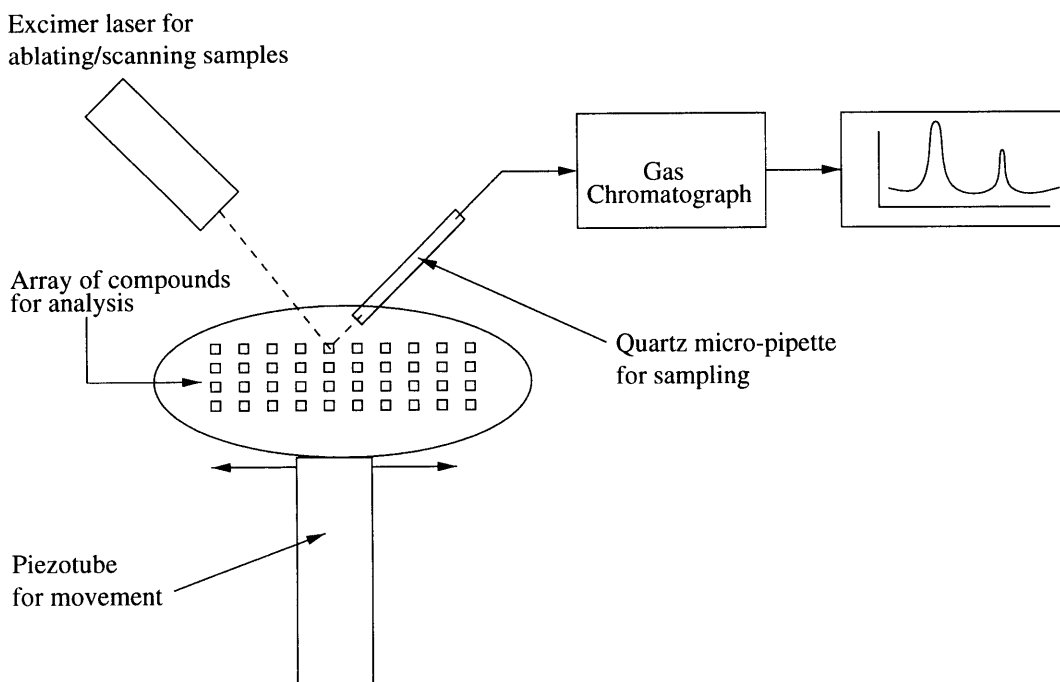


Figure 3-7: Pharmaceutical application.

column may be used in conjunction with a detector (e.g., Raman spectrometer) to enhance the characterization of complex compounds or mixtures. All in all, many possible areas of application can be seen for excimer laser ablation. An attempt is made in this thesis to use excimer laser ablation as a material characterization tool by studying the effects of ablation frequency, time, and sample volume for different high molecular weight materials. This effort is described in Chapter 5.

Chapter 4

Manufacturing of Quartz

Micro-Columns

4.1 Introduction

As mentioned in Chapter One, the two goals of this thesis are first, to develop a quartz micro-column manufacturing technique and second, to investigate the use of excimer laser ablation for the characterization of high molecular weight materials. This chapter deals with the manufacturing of quartz micro-columns. Figure 4-1 shows the schematic of the method being investigated to manufacture quartz micro-columns. The setup consists of a quartz column held in place by a stationary end and a Lorentz-force linear actuator using tube fixtures. The column is softened using a CO_2 laser and then pulled quickly by the actuator which is driven by an amplifier as shown. The goal of this work is to manufacture small diameter micro-columns which may be used as sampling devices such as the one shown in Figure 3-7. These micro-columns are by no means limited to this type of application, and other useful tools which use them may be foreseen. For instance, with some changes to the manufacturing setup one may be able to make micro-columns for gas chromatography, using a relatively cheaper technology and with a smoother geometry compared to the past efforts mentioned in Chapter 2. The following sections describe each of the components in the experimental setup, and the manufacturing process involved in the making of the quartz micro-

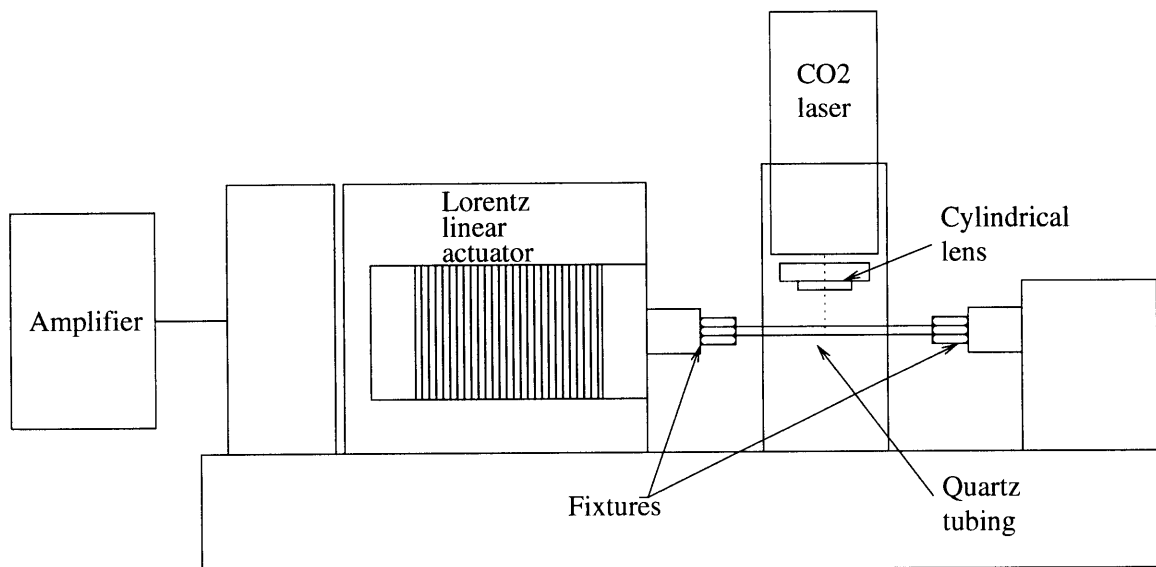


Figure 4-1: Micro-column manufacturing setup.

sniffers.

4.2 Lorentz Linear Actuator

The Lorentz-force linear actuator ($0.45\text{ m} \times 0.195\text{ m} \times 0.165\text{ m}$) used in the setup consisted of a motor coil which runs on a linear guide resting on several adjustable roller bearings. These bearings were adjusted by tightening and loosening several adjustment bolts found along the linear guide so as to provide the smoothest movement possible. The actuator was bolted onto a vertical aluminum beam of rectangular cross-section.

The fixtures used to attach the quartz column for pulling consisted of NPT-type (National Pipe Threading) tubing fixtures with Teflon ferrules. An aluminum threaded rod at the end of the actuator served as the link between the actuator and a tubing fixture to attach one end of the quartz column. The other end was attached to a fixed support as shown in Figure 4-1. The fixed support consisted of a small piece of rectangular cross-section aluminum tubing and an L-shaped bracket onto which a fixture, similar to the one used for the actuator, was attached. The original setup consisted of larger diameter fixtures and in order to accommodate the smaller diam-

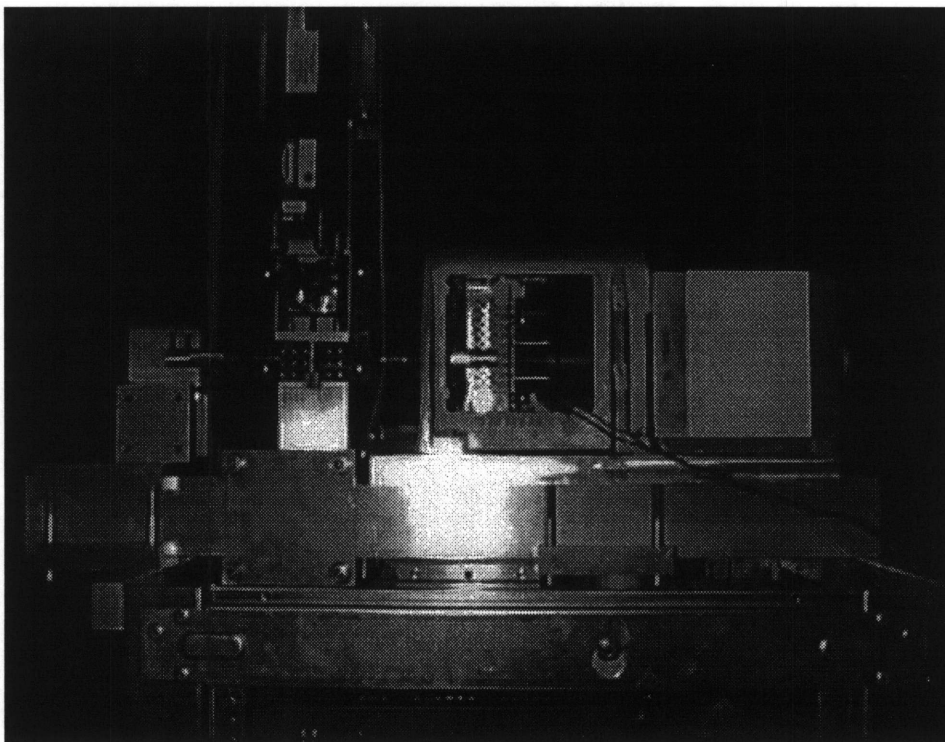


Figure 4-2: Photograph showing micro-column manufacturing setup.

eter quartz tubing, a smaller set of fixtures was attached via a small piece of copper tubing. This gave the setup some needed mechanical compliance which prevented too many episodes of column fracture. Figure 4-2 shows a picture of the actual setup.

4.3 Amplifier Circuit.

The major component of the amplifier circuit (see Appendix C) used consisted of a high-capacitance Maxwell capacitor ($193 \mu F$) which may be charged up to $1000 V$. The discharge of the capacitor allows for quick movement of the Lorentz actuator and pulling of the quartz column. The rest of the circuit consists of a low-pass filter at the power input, a volt meter to measure the capacitor voltage, and a bridge rectifier circuit for the power supply. The circuit allows for manual discharge of the capacitor by pressing a switch as well as computer control.

The maximum energy that can be generated to pull the quartz columns with this

setup can be estimated using

$$E_C = \frac{1}{2}CV^2 \quad (4.1)$$

which amounts to $10^4 J$ if the Maxwell capacitor's capacitance and maximum voltage are used. An approximation of the initial acceleration possible can be made by using the force generated by the motor equation [42] which is given by

$$F = Bli \quad (4.2)$$

where B is the magnetic field in the actuator's air gap, l is the coil length, and i is the current going through the coil. The length of the coil can be calculated knowing the number of turns in the coil N , and the diameter D of the coil:

$$l = N \times \pi D \quad (4.3)$$

The number of turns in the coil is 92, while the diameter was measured to be 92 *mm*. If these are substituted into Equation 4.3, the coil length is found to be 26.59 *m*. The force generated by the actuator can now be written in terms of the coil current if we substitute in the magnetic field in the actuator's air gap which was measured to be 0.65 *T*:

$$F = 17.2834i \quad (4.4)$$

An estimate of the initial current can be made if it is assumed that initially the coil's inductance acts like a short. The current can then be calculated using the input voltage and the coil's resistance (measured to be 2 Ω):

$$i = \frac{V}{R} = \frac{1000V}{2\Omega} = 500A \quad (4.5)$$

Now that the current is known, the actuator force can be calculated using Equation 4.4 which yields 8641.7 *N*. Finally, using the mass of the coil (which was measured to be 275 *g*), the maximum initial acceleration is found to be $3.14 \times 10^4 \frac{m}{s^2}$. Of course, these calculations assume no losses due to friction and other dissipation factors which

means the acceleration is less than this.

4.4 CO_2 Laser Setup and Optics

The CO_2 laser used was a water-cooled 10 W Synrad Inc. laser mounted on a vertical aluminum tube of rectangular cross-section. A 5 VDC input to the laser was supplied. The optics used for the laser focusing consisted of a 25×12 mm $ZnSe$ cylindrical lens with focal length of 25 mm and refraction index of 2.4 which allowed for focusing of the laser beam into a line. The lens was mounted on a three degree-of-freedom lens mount. The lens mount was in turn mounted on a micrometer stage which allowed for vertical movement of the lens to adjust the focused beam.

The selection of the CO_2 laser as a heat source was due to the cleanliness of laser heat [43]. CO_2 laser heat does not leave an evaporative metal residue on the quartz tubing as conventional metal filaments may. If the laser is programmed, the user may program the amount of power to be supplied to the glass, and define the pattern of heat distribution along the glass. In addition, the laser does not leave residual filament heat, that is, when the laser is turned off, heat delivery to the quartz stops instantly, hence eliminating the need for an air jet cooling system. Furthermore, a laser does not have the problems of a hydrogen flame in terms of non-unidirectionality and inability to modulate.

4.5 Quartz As a Column Material

The decision to use quartz as a column material is a result of the superior and unique properties that it offers [36] (see Table 4.1). Quartz, also known as fused silica, has the smallest known coefficient of thermal expansion of any pure material ($5.5 \times 10^{-7} K^{-1}$). In addition, quartz may be drawn into long, thin fibers with very low internal damping, and a linear twisting stress-strain relation to the breaking point. Quartz fibers are very strong. For example, a quartz fiber 0.254 mm in diameter has a tensile strength of 344.74 MPa; a fiber 0.0254 mm in diameter a strength of at least

689.48 MPa; and a fiber of 0.00254 mm in diameter a strength in excess of 6.8948 GPa. Springs using quartz fibers provide the best possible realization of Hooke's law.

Property	Value
Density	$2.2 \times 10^3 \frac{kg}{m^3}$
Annealing point	1410°K
Hardness	4.9 Moh's scale
Tensile strength	$4.8 \times 10^7 \frac{N}{m^2}$
Electrical resistivity	$10^{7.5} \Omega - m$ (623°K)
Compressive strength	$> 1.1 \times 10^9 \frac{N}{m^2}$
Dielectric constant	3.75 (293°K and 1 MHz)
Bulk modulus	$3.7 \times 10^{10} \frac{N}{m^2}$
Rigidity modulus	$3.1 \times 10^{10} \frac{N}{m^2}$
Strength	$1.6 \times 10^7 \frac{V}{m}$
Young's modulus	$7.17 \times 10^{10} \frac{N}{m^2}$
Poisson's ratio	0.16
Coefficient of thermal expansion	$5.5 \times 10^{-7} \frac{m}{m \cdot ^\circ K}$ (293°K-593°K)
Index of refraction	1.4585
Thermal conductivity	$1.4 W \frac{m}{m^2 \cdot ^\circ K}$
Specific heat	$750 \frac{J}{kg}$
Fusion temperature	2070°K
Softening point	1940°K

Table 4.1: Properties of clear fused quartz (Adapted from Bolz et al, 1973 [44]).

For instance, torsion springs and coil springs made of a quartz fiber are usually used in delicate laboratory balances. Furthermore, quartz retains its excellent mechanical properties up to 1073°K.

Aside from its mechanical properties, fused silica also provides excellent chemical durability [36]. Fused silica is so stable that a white-hot piece can be immersed in liquid air without fracturing. Being a type of glass, it does not have a melting point. Optically, quartz is transparent over the widest wavelength range. Also, quartz is virtually free from fluorescence when illuminated.

In terms of electrophysiological research, quartz provides excellent properties [43]. Quartz pipettes can pierce through tough tissue that would otherwise break conventional pipettes. Thin-wall quartz can form tips that can penetrate cells as can thick-wall borosilicate, yet the thin-wall quartz will have a larger pore size and there-

fore lower resistance. Quartz also provides desirable electrical properties in terms of a low dielectric constant, a low loss factor and a volume resistivity that is orders of magnitude greater than borosilicate. These properties give quartz superior noise performance when compared to pipettes made from other glass. With the exception of quartz, all common glasses incorporate metal ions to decrease their melting point. By eliminating these metal ions, recording artifacts and alteration of channel kinetics may be minimized. Because of its mechanical, refractory, and chemical properties, quartz is a very desirable material. Fused quartz from Mid-Rivers Glassblowing, Inc. in St. Charles, Missouri was used for the manufacturing of micro-columns.

4.6 Manufacturing of Quartz Micro-columns

The manufacturing of micro-columns using quartz tubing involved the installment of quartz columns using the fixtures in the setup, softening of the columns using the CO_2 laser and the drawing of the column using the actuator. Column initial diameters ranged from 0.3 *mm* to 1 *mm*. After successful installation of the column, the amplifier system was charged up to a specified voltage. The CO_2 laser was turned on and focused just beside the quartz column at first since the focused beam was able to soften the tubing quite easily (especially the smaller diameter tubing), and cause the columns to bend under their own weight. Once the laser was turned on and the amplifier system charged up, the focused beam was slowly moved onto the column's surface using the lens mount adjustment knobs until column softening was observed. At this point the capacitor was discharged manually by pressing the switch on the amplifier which then caused the quick movement of the actuator and thus the drawing of the column.

There were several issues involved in the manufacturing process. These and other results will be discussed in Chapter 6.

Chapter 5

Excimer Laser Ablation Product Sampling and Analysis

5.1 Introduction

The second part of this thesis was to demonstrate the sampling and analysis of high molecular weight materials using excimer laser ablation and gas chromatography. Figure 5-1 shows the setup used to carry out these experiments. The setup consisted of an excimer pulsed laser, a fused silica focusing lens and a gas-collection cell attached to a stepper motor X-Y stage for movement. All of these components rested on a small optical bench inside a clean room. The gas analysis was carried out using a gas chromatograph model 6890 by Hewlett-Packard Analytical in San Fernando, California. The following sections describe each of the components in more detail as well as the procedure involved in the experiments.

5.2 Excimer Laser and Optics

The excimer laser used for the ablation of materials was an MPB Technologies, Inc. *KrF* laser model PSX-100. The wavelength of the laser was given as 248 *nm* and the gas mixture used was a fluorine, krypton, neon mix. The total fill pressure used was 0.8 *MPa* and the maximum pulse energy was 6.5 *mJ*. The laser allows for

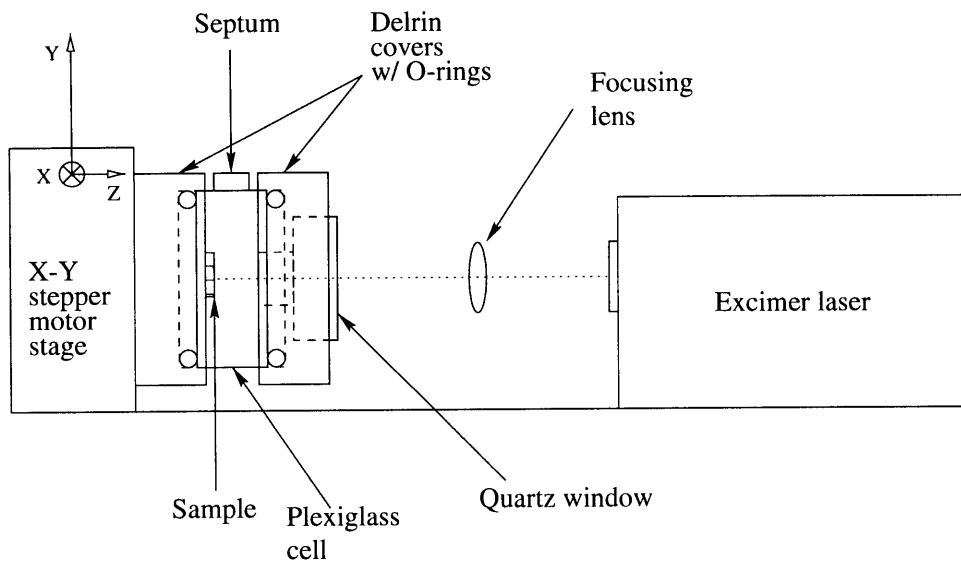


Figure 5-1: Excimer laser ablation sampling and analysis setup.

variation of the pulsing rate from 10 to 102 Hz , and the maximum average power at 102 Hz is given as 560 mW . The beam dimensions and divergence were given as $3 \times 3.9 \text{ mm}$ and $5.1 \times 5.5 \text{ mrad}$, respectively. The optical setup consisted of a fused silica focusing lens mounted on an L-bracket which was bolted on a three degree-of-freedom micrometer stage that allowed for adjustment of the focused laser pulses.

5.3 Gas Collection Cell

The gas-collection cell was made by machining two square pieces of homopolymer acetal resin (also known as Delrin) with two circular grooves (see Figure 5-1). In addition, a circular section was machined on one of the square pieces in order to place a quartz window to allow for the transmission of the excimer laser radiation while at the same time trapping the ablation gas products. Quartz is transparent to UV radiation as mentioned in Chapter 4. A third piece consisted of an acrylic estermonomer (also known as Plexiglas) ring which was sandwiched between the Delrin square pieces' circular grooves with two O-rings in order to have a good seal. The Plexiglas ring piece has a rubber septum inlet attachment through which gas collection took place with a gas-tight syringe. This inlet consisted of a tubing male/female connector which

was screwed on the Plexiglas ring. Detailed drawings of the gas collection cell can be found in Appendix A.

5.4 Gas Chromatograph

As mentioned before, the gas analysis was carried out using an HP 6890 gas chromatograph (GC) with electronic pneumatic control and a flame ionization detector (FID). The GC also allows for split and splitless injections, and temperature and gas flow programming. The column used was an siloxane HP-5MS capillary column. Nitrogen was used as the carrier and makeup gas, while hydrogen and air were used for the FID. The software used for the data acquisition and analysis was the ChemStation software provided by HP. The software allows for data acquisition, analysis in terms of chromatographic peak integration and component identification after appropriate instrument calibration, as well as other useful operations.

5.5 Excimer Laser Ablation Experiments

The excimer laser ablation sampling and analysis experiments involved the ablation of a material sample, the sampling of the ablation products using a gas-tight syringe, and their introduction into the gas chromatograph for analysis. All of these operations were done manually. The first step which was necessary before any experiments could be carried out was to optimize the gas chromatograph settings to obtain reasonable gas separations. This involved variation of the column oven temperature, in particular, as well as the flow rate of the carrier gas. After some trial runs were made, the GC settings in Appendix C were used for all of the experiments. After setting the GC settings, an air sample was injected to make sure that the experiments showed actual ablation gas products and not air components. Once this was done, the following sets of experiments were carried out.

5.5.1 Influence of Pulse Rate

The first set of experiments was based on the variation of the excimer laser pulse rate or frequency. This consisted of setting the rate at four different settings ranging from 10 to 100 *Hz* for each experiment. The injection volume for these experiments was 0.3 *ml*. For each experiment the excimer laser was turned on after setting the correct pulse frequency. The material was then ablated for 40 seconds while the gas-collection cell containing the sample was manually moved latitudinally and longitudinally using the X-Y stepper motor knobs. After 40 seconds of ablation, a gas sample was drawn using a gas-tight syringe through the rubber septum in the region just above the ablated area to ensure that the gases being collected represented a good sample of the ablation products. This is based on past efforts which have shown that during the ablation of polymers a plume forms just above the ablating surface [45]. Once a sample was taken, it was introduced into the gas chromatograph and the GC method was initialized. After each ablation/gas collection event, the gas cell was allowed to ventilate by removing the septum inlet to ensure similar initial conditions for each experiment.

5.5.2 Influence of Injection Volume

The second set of experiments was based on the variation of the injection volume. This consisted of drawing different injection volumes ranging from 0.1 to 0.6 *ml* using the gas-tight syringe. The ablation time for these experiments was 40 seconds. The excimer laser pulse repetition rate used for all of these experiments was 100 *Hz*. The same procedure of ablation and gas collection described in the previous section was then repeated for each experiment except that for each experiment a different sample volume was sampled. The gas volume was measured using the gas-tight syringe's gradations.

5.5.3 Influence of Ablation Time

The third set of experiments was based on the variation of ablation time. This consisted of allowing the ablation time of the material to vary from 60 seconds to 120 seconds. The injection volume for these experiments was 0.3 *ml*. The excimer laser pulse repetition rate used was 100 *Hz*. For each experiment the material was ablated for a different length of time and then gas sampling and analysis was carried out.

5.5.4 Variation According to Material

The three sets of experiments just described were carried out by first using a polyethylene polymer blend (commonly known as SaranWrap which is manufactured by Dow Chemical). In order to observe the difference in results when using a different material, these sets of experiments were then repeated using high-density polyethylene as a second material. The SaranWrap was folded into a rectangular piece to be able to fit it into the gas-collection cell. The polyethylene consisted of a rectangular piece cut from a high-density polyethylene rod.

5.5.5 Calibration of Gas Chromatograph

The gas chromatograph was calibrated by introducing individual sample compounds into the chromatograph under the same conditions as the experiments were carried out. The selection of calibration compounds was based on past efforts' results as discussed in Chapter 3 [39, 40, 41]. The compounds included carbon monoxide, carbon dioxide, ethane, methane, and propane, benzene, and toluene. The liquid standards were introduced using a microsyringe. The gas samples required more effort for introduction into the GC. Each gas was introduced from a laboratory size cylinder into a gas bag which was then punctured with a gas-tight syringe to collect a sample of the gas. Each gas was introduced into the GC a few times to ensure repeatability of the measurements. After calibration, the identification of the ablation components in the experimental results was attempted. The results and observations for all of the experiments just described will be the subject of the next chapter.

Chapter 6

Results

The following sections present the results for both the quartz micro-column manufacturing development and the excimer laser ablation products sampling and analysis.

6.1 Quartz Micro-Column Manufacturing

As mentioned in Chapter 4, the manufacturing of micro-columns using quartz tubing involved the installment of a quartz column on the fixtures, the softening of the columns using the CO_2 laser, and the drawing of the column using the actuator. Some micro-columns were made using this technique. Figure 6-1 shows a scan of two of these columns. The bottom column shown had an initial outer diameter of 0.44 mm . The capacitor voltage used to draw it was 100 V and the final length was 20 mm . The top column's initial outer diameter was 0.43 mm . The capacitor voltage used to draw it was 150 V , and the final micro-column length was 31.75 mm . Just from these results, it appears that the length of each column increased with capacitor voltage as it would be expected.

One of the initial problems in the manufacturing process was the quartz column diameter size. Initially, quartz column diameters in the 1 mm range were being used. These were difficult to soften with the CO_2 laser being used. Smaller columns in the range of 0.5 mm outer diameter were used to be able to soften them. The micro-columns made showed great robustness in terms of strength. The fibers could be

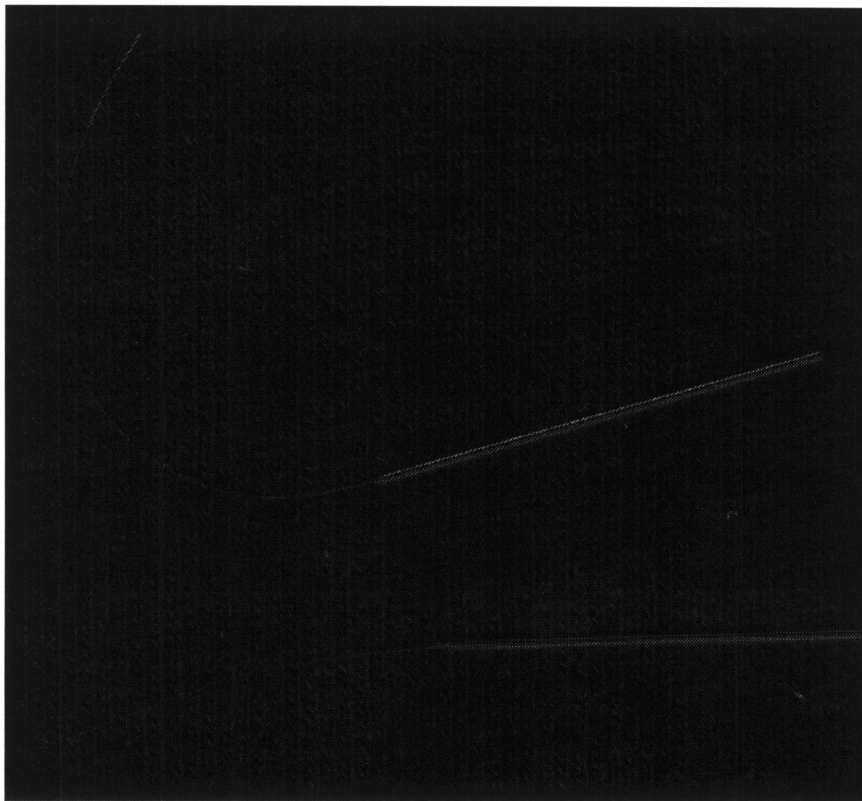


Figure 6-1: Photograph showing two quartz micro-columns.

plucked and bent without any mechanical failure. The major problem in the process was the alignment and tightening of the quartz columns prior to drawing them. The initial columns' brittleness was a major obstacle when trying to tighten the fixtures which held them. Another problem was the distortion of the Teflon ferrules when the fixtures were being tightened which caused many of the columns to fracture. Aside from these difficulties, some micro-columns were manufactured. Their outer diameters were reduced by at least a factor of ten when observed under a light microscope and their inner diameters were obviously smaller in size. One of the experiments carried out to demonstrate the hollowness of the columns was to immerse them in water. After doing so, water went up the columns due to capillary action as expected. The cross-section at each end of the columns was also observed under a light microscope which indeed verified their hollowness. It appeared that the columns were hollow throughout their length when observed under the light microscope but verification using a scanning electron microscope should be carried out to verify this.

6.2 Excimer Laser Ablation Products Sampling and Analysis

The excimer laser ablation sampling and analysis experiments involved the ablation of SaranWrap and polyethylene, the sampling of the ablation products using a gas-tight syringe, and their introduction into the gas chromatograph. The following sections review the results for each of the sets of experiments described in the previous chapter.

6.2.1 General Results

The experimental results for the excimer laser ablation products sampling and analysis experiments showed very intriguing features. The first of these was the fact that in general, components of each ablated material tended to increase in concentration with increasing ablation rate for both the SaranWrap and polyethylene (see Figures 6-2, 6-5). In addition, the concentration also increased with injection volume for both materials (see Figures 6-3, 6-6). The concentration was generally unaffected as a function of ablation time in the case of the SaranWrap (Figure 6-4), but it increased in the case of polyethylene (Figure 6-7). The ablation experiments on the SaranWrap yielded three major components in general. These are labeled A, B, and C in Figures 6-2 through 6-4. The polyethylene experiments yielded four. These are labeled A, B, C, and D in Figures 6-5 through 6-7. The difference in component number was probably due to the different material makeup, and the different interactions between the laser pulses and each material. In terms of designing a useful device using this technique, this is very promising since with greater care one may be able to implement a far more controlled device in terms of the ablation and sampling volume which would provide enough criteria for differentiating between various materials. Another aspect of the results is the similarity between the chromatograms' shapes and retention times for both the SaranWrap and polyethylene. This is probably due to the fact that SaranWrap and other plastic food wraps are thought to be based on

polyethylene polymer blends [46].

There was some slight variation in some of the components' retention times from experiment to experiment (Figures 6-8 through 6-13). One of the major causes of this variation in the retention time was probably due to the fact that a lot of the tasks in the experimental process were done manually. One of these tasks was the sampling of the ablation gases and their introduction into the gas chromatograph. In particular, when introducing a sample into the gas chromatograph, the start button on the instrument had to be pressed once the injection was made. Even though an attempt was made to be consistent for each chromatographic analysis, there was probably some variation in time due to human error which affected the retention times for each separation. In addition, there was probably some variation in the injection volume when sampling ablation products from the gas-collection cell since this was a manual operation. In general, gas-tight syringes are prone to reading errors ($< 1\%$) and leakage [47]. This leakage is due to the increased pressure that the syringe experiences when inserted into the chromatograph's septum. Initially, the carrier gas rushes through the needle into the syringe volume until the pressure reaches that of the head of the column. Even the smallest leak between the barrel and plunger may cause a significant sample loss as a result of the increased pressure.

Another source of error was the integration process. As mentioned before, the integration of the chromatographic peaks was done using the HP software. The integration affected the retention times because the retention time is measured at the top of the peaks which were wide at times. A better indication of retention time is the start of each peak since this is when each component starts to exit the column.

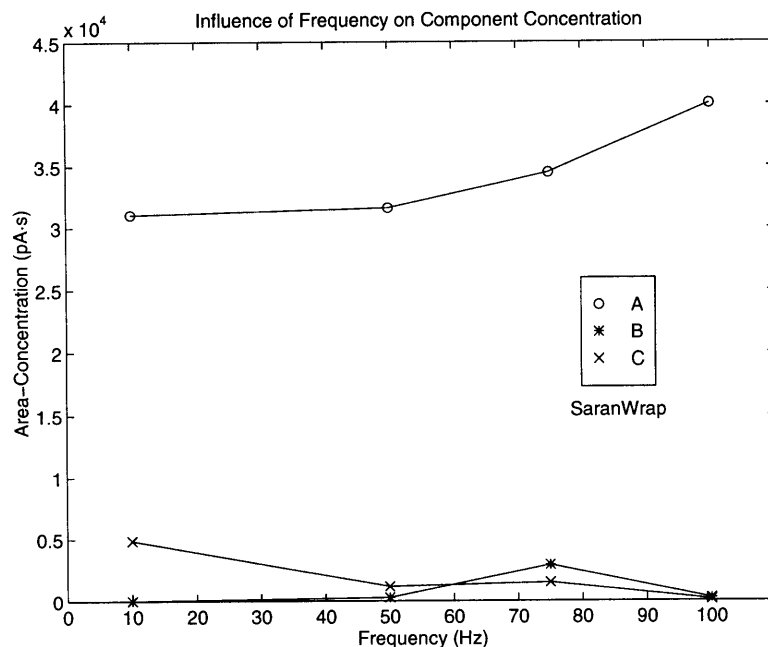


Figure 6-2: Influence of excimer laser pulse frequency on component concentration for SaranWrap. Concentration of the three major components (A, B, C) of the ablation gases shown. Ablation time was 40 s and injection volume 0.3 ml.

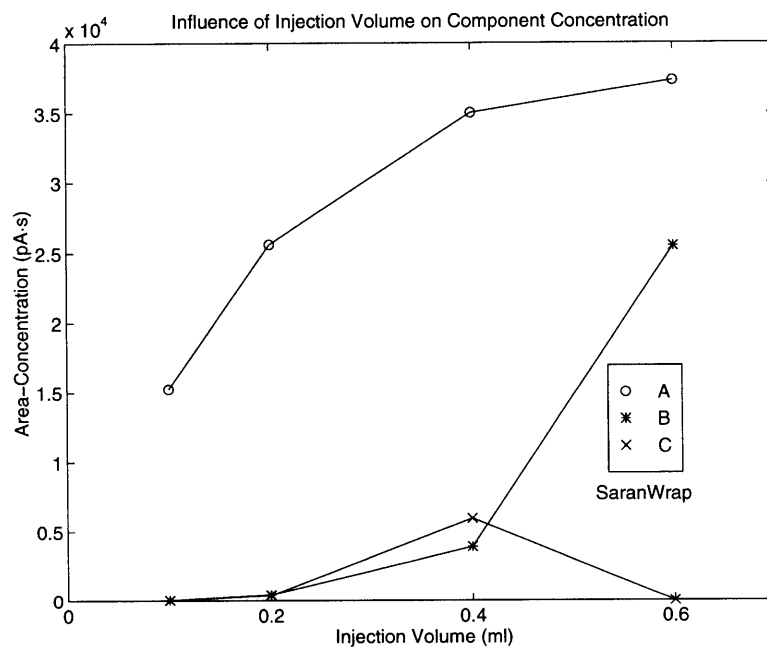


Figure 6-3: Influence of injection volume on component concentration for SaranWrap. Ablation frequency of 100 Hz and ablation time of 40 s.

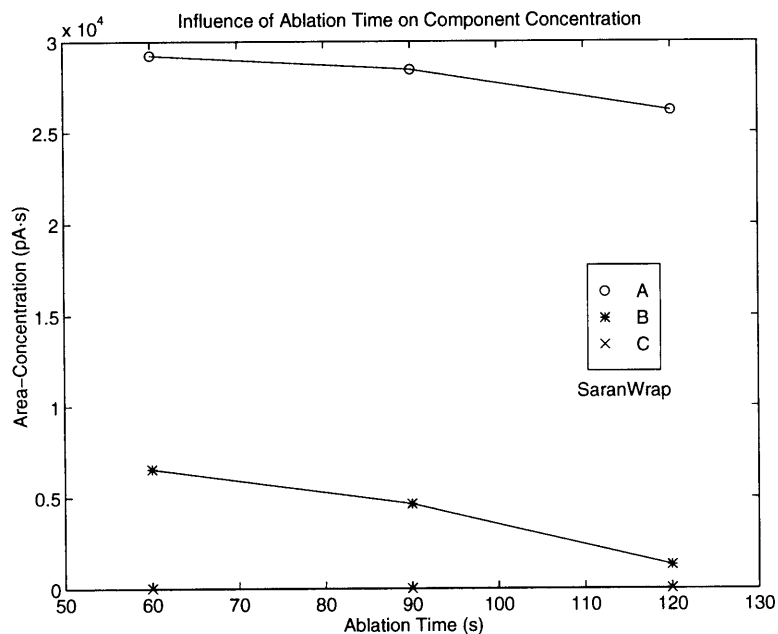


Figure 6-4: Influence of ablation time on component concentration for SaranWrap. Ablation frequency of 100 Hz and injection volume of 0.3 ml.

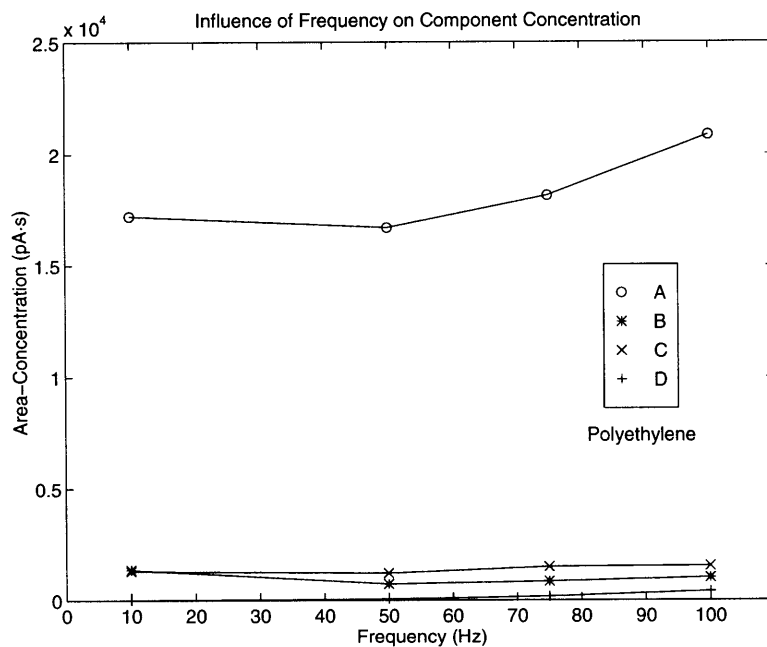


Figure 6-5: Influence of excimer laser pulse frequency on component concentration for polyethylene. Four major components (A, B, C, D) of ablation gases shown. Ablation time was 40 s and injection volume 0.3 ml.

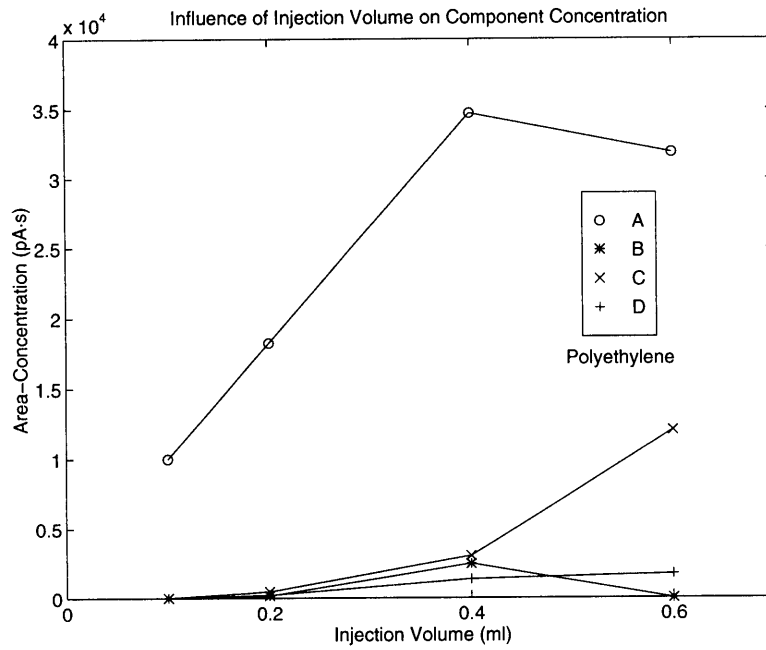


Figure 6-6: Influence of injection volume on component concentration for polyethylene. Ablation frequency of 100 Hz and ablation time of 40 s.

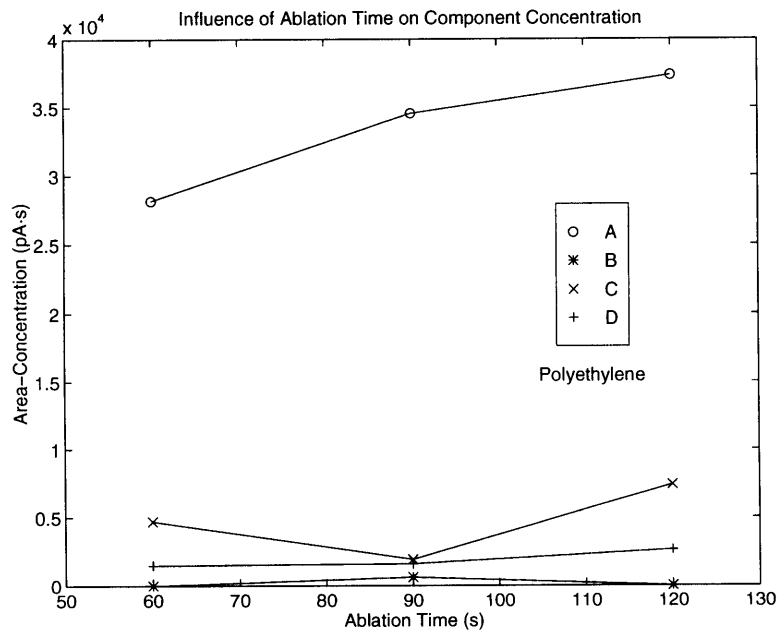


Figure 6-7: Influence of ablation time on component concentration for polyethylene. Ablation frequency of 100 Hz and injection volume of 0.3 ml.

6.2.2 Influence of Repetition Rate on Concentration

The influence of the pulse frequency for the SaranWrap experiments showed some interesting features (see Figure 6-8). First, there were in general three major components found in the ablation gas products. At 10 *Hz* there appears to be only two components in the gas mixture, occurring at times 82.8 and 100.2 seconds. As the pulse frequency is increased though, the GC output clearly shows the third component occurring at time 84 seconds in the mixture which may indicate that the higher pulse rate allowed the laser to break up the material's surface to a greater extent. In general, the higher the frequency used, the higher the components' concentration (Figure 6-2). This behavior was mostly evident for the major component A which increased with each increase in pulse frequency in a roughly linear fashion. The minor components increased in concentration at times but decreased at others. This may be due to several factors, including sample leakage during injection or the variation in gas sampling from the gas-collection cell.

6.2.3 Influence of Injection Volume on Concentration

The influence of the injection volume for the SaranWrap experiments also demonstrated intriguing results (see Figure 6-9). The first experiment using 0.1 *ml* of injection volume yielded the major component A as before but only a much smaller second component which may indicate that the injection volume was too low and didn't include enough of the other three components' concentration to have shown up in the chromatogram. As the volume was increased to 0.2 *ml*, one can see the three components present as before, but once the volume is increased to 0.4 and 0.6 *ml*, peak broadening of the two minor components occurs which causes them to overlap. There seems then to be an optimal injection volume around 0.2 *ml* which results in the highest resolution. For these experiments the concentration of the components increased with injection volume in general (Figure 6-3).

6.2.4 Influence of Ablation Time on Concentration

The influence of the ablation time for the SaranWrap experiments showed that, in general, the ablation time did not affect the components' concentration (see Figures 6-10, 6-4). This may be a result of the material's composition or the gas sampling. The only considerable effect was the presence of a small fourth component which may have been a result of the increased ablation time. The increased ablation time may have allowed the laser to further break down the material and may explain the presence of the smaller fourth component.

6.2.5 Variation According to Material

The influence of the pulse frequency for the polyethylene experiments demonstrated some of the same characteristics shown by the SaranWrap results (see Figure 6-11). Again, the components' concentration increased, in general, with the pulse frequency, especially for the major component A (Figure 6-5). The increase in concentration was not as sharp as the SaranWrap case though. The major difference for these experiments was the presence of a fourth component as opposed to three for the SaranWrap case. The fourth component occurred at 79.8 seconds and may be due to the different composition of polyethylene.

The influence of the injection volume for the polyethylene experiments again showed (see Figure 6-12) similar results to the SaranWrap results. At an injection volume of 0.1 *ml* there are only two components present, mostly the main component A. As the volume is increased to 0.2 *ml*, the four components appear as before. Then as the injection volume is increased to 0.4 and 0.6 *ml*, again peak broadening and overlap of the three minor components occurs. Again, there seems to be an optimal injection volume for the polyethylene case which lies around 0.2 *ml*. For these experiments the concentration of each component increases with volume in general (see Figure 6-6).

The influence of the ablation time for the polyethylene experiments (see Figure 6-13) showed different results compared to the SaranWrap case. The components'

concentration did increase with the ablation time (see Figure 6-7). The increased ablation time appears to have allowed further breaking down of the polyethylene which caused an increase in each of the components' concentration.

6.2.6 Identification of Ablation Products

The GC calibration results showed that the only gases present in the experimental results out of the ones used for the calibration were methane, propane, and ethane. The calibration results for benzene, toluene, carbon monoxide and carbon dioxide showed retention times greater than the ones observed in the experiments. This shows that these were not present in the analysis or in very negligible quantities. The calibration results using methane, propane and ethane indicate their presence in the ablation gas products. In order to fully verify this a GC-Mass Spectrographic analysis should be carried out. Another observation worth mentioning is that during each of the experiments the plume described in past efforts was observed as the ablation of the material took place. One of the after effects was a black residue along the inner surfaces of the gas-collection cell. This black residue may be a sign of carbon as observed and confirmed in past efforts [41].

The following pages contain the individual results for each experiment. Appendix D contains the file names and integration results for each of them.

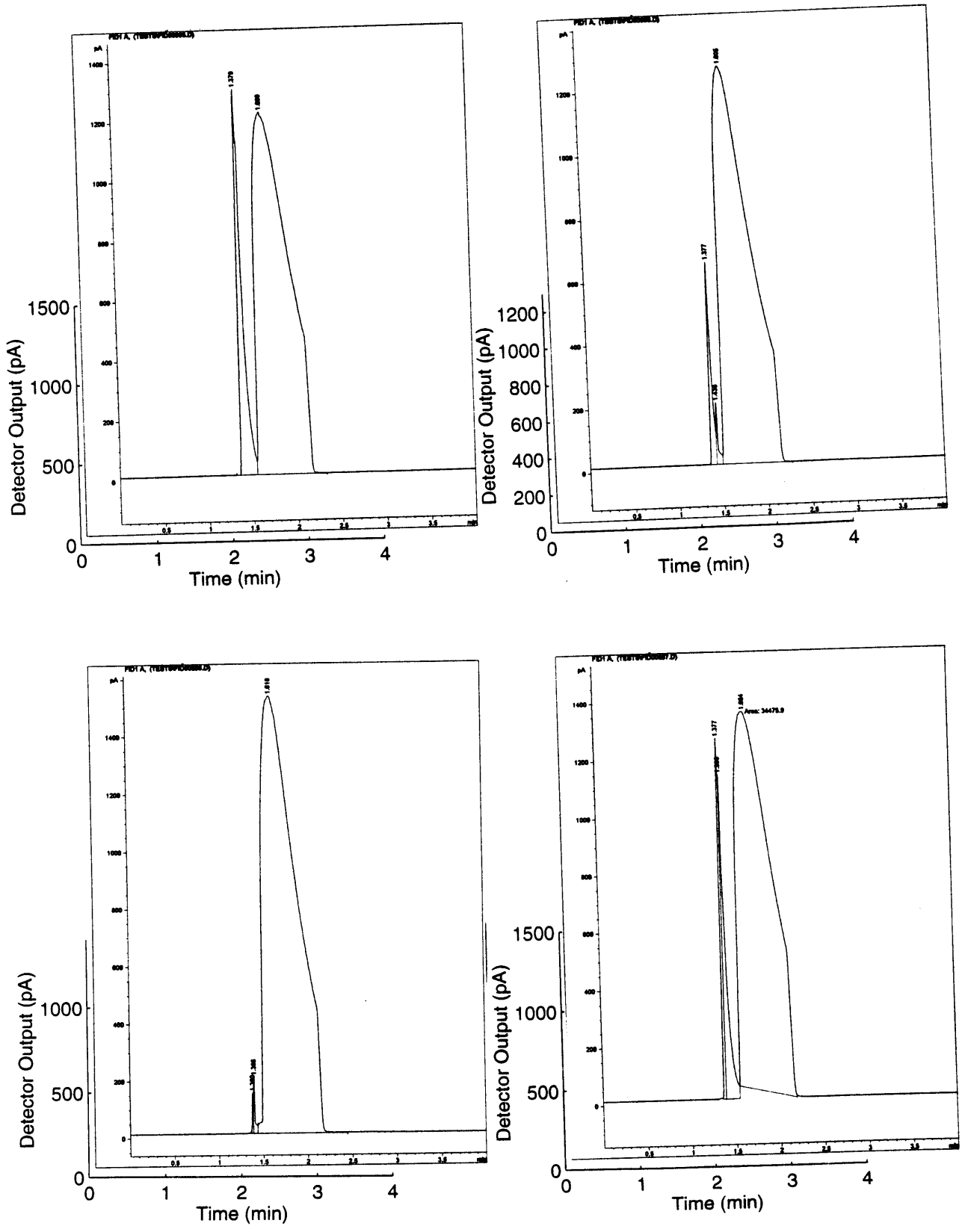


Figure 6-8: Results for pulse frequency variation experiments for SaranWrap. Clock-wise starting from the top left corner: 10 Hz, 50 Hz, 75 Hz, and 100 Hz.

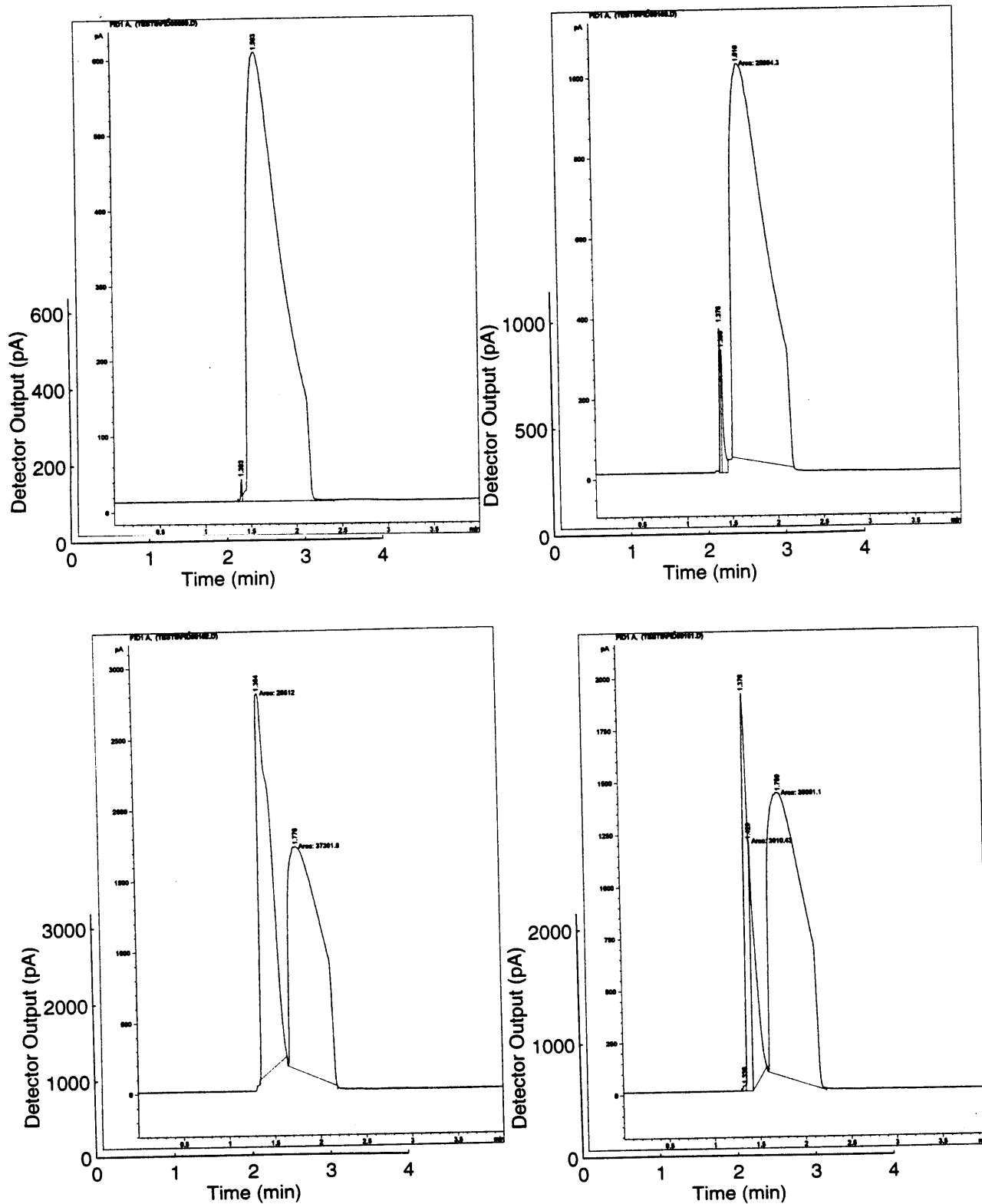


Figure 6-9: Results for injection volume variation experiments for SaranWrap. Clock-wise starting from the top left corner: 0.1 ml, 0.2 ml, 0.4 ml, and 0.6 ml.

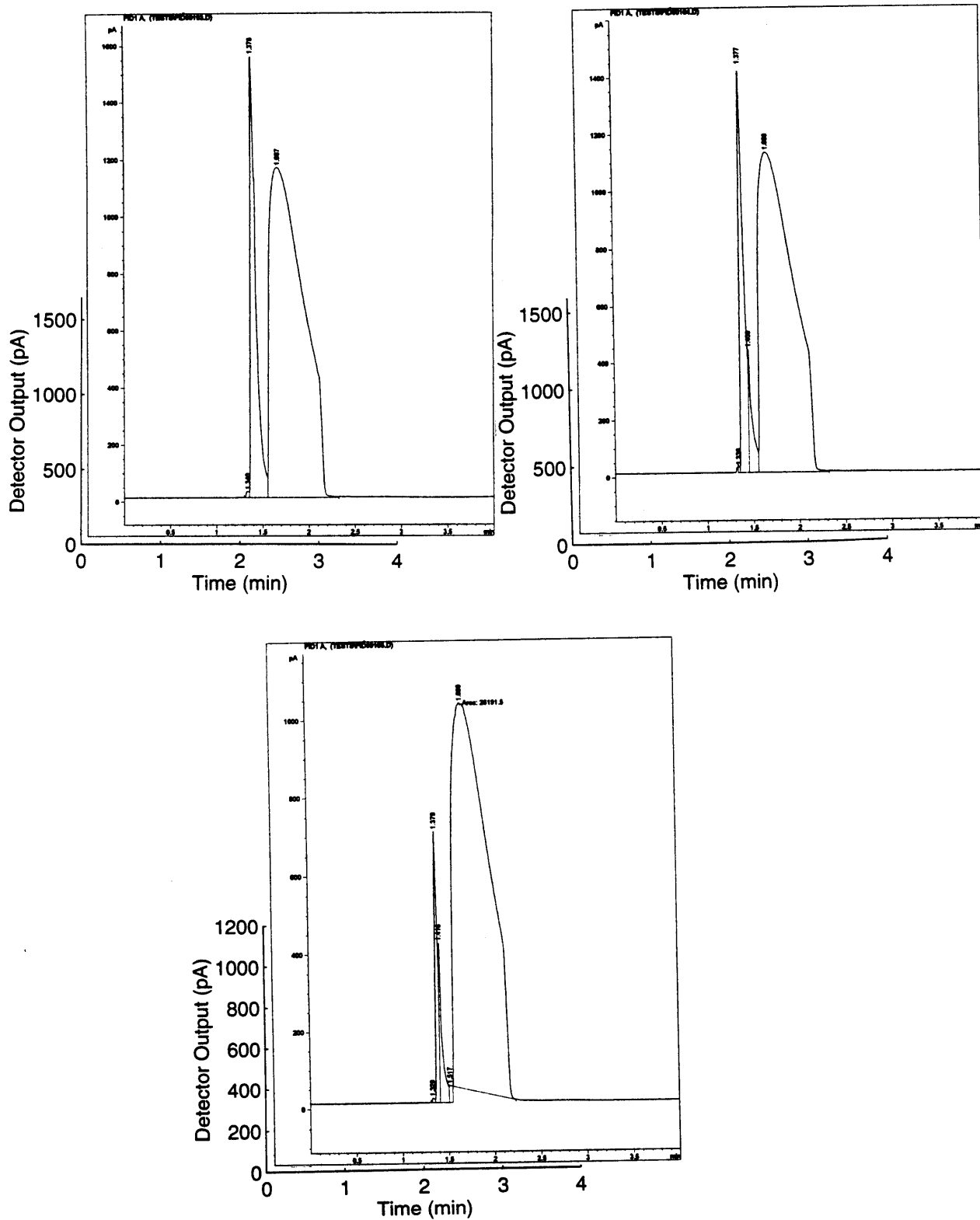


Figure 6-10: Results for ablation time variation experiments for SaranWrap. Clockwise starting from the top left corner: 60 seconds, 90 seconds, and 120 seconds.

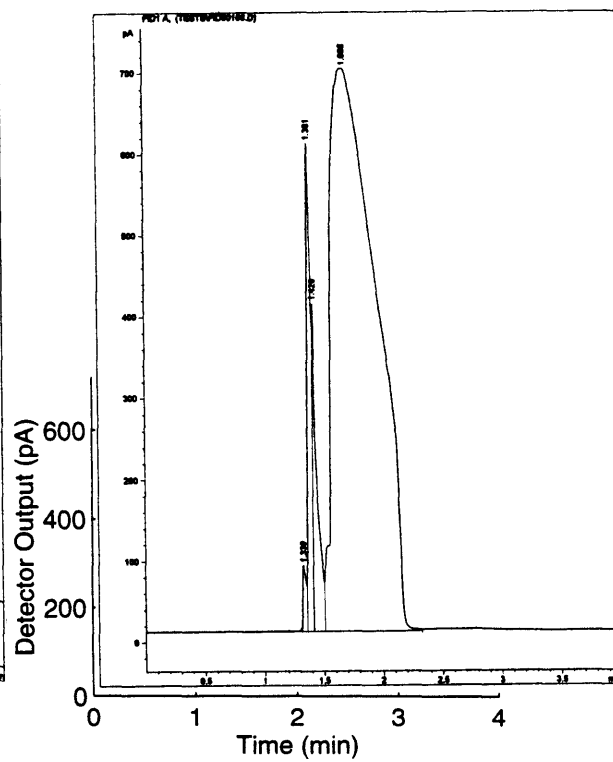
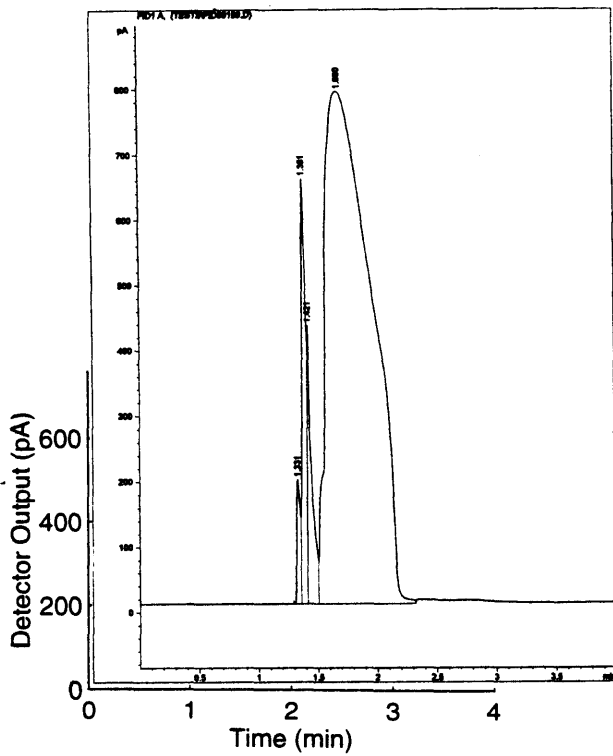
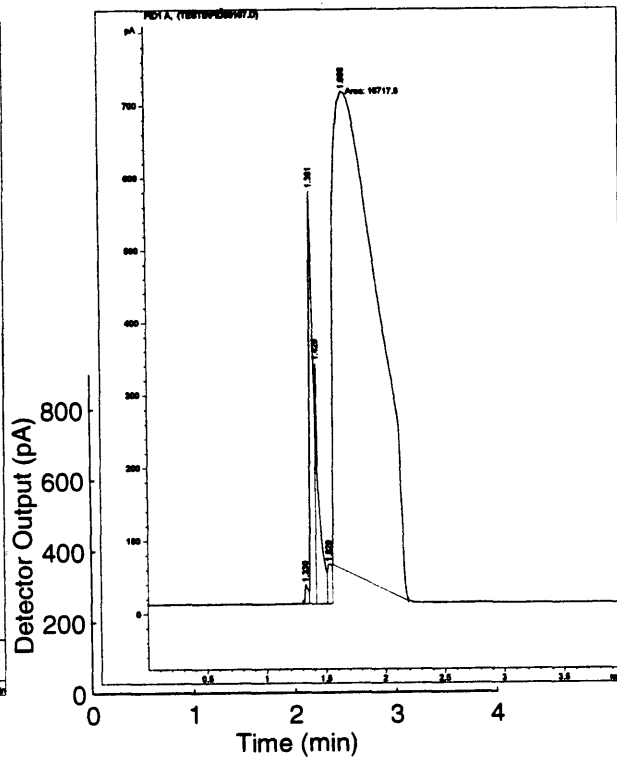
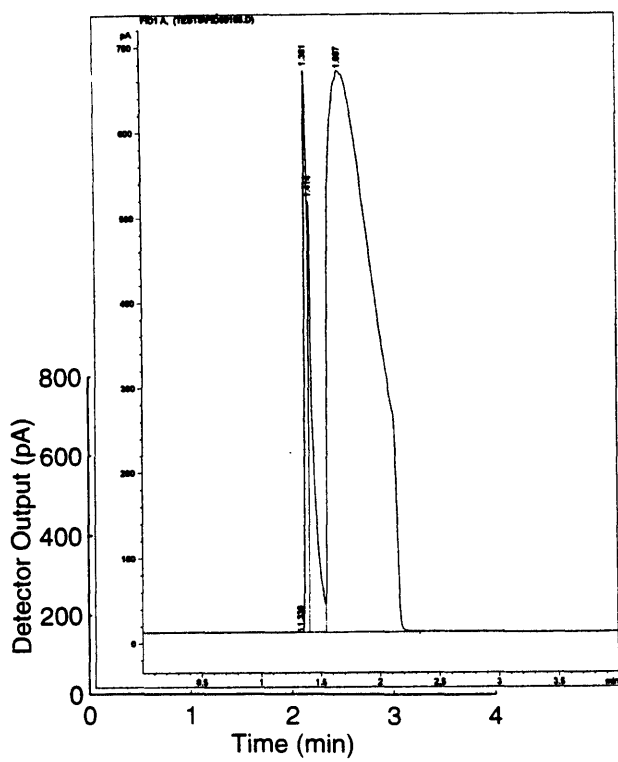


Figure 6-11: Results for pulse frequency variation experiments for polyethylene. Clockwise starting from the top left corner: 10 Hz, 50 Hz, 75 Hz, and 100 Hz.

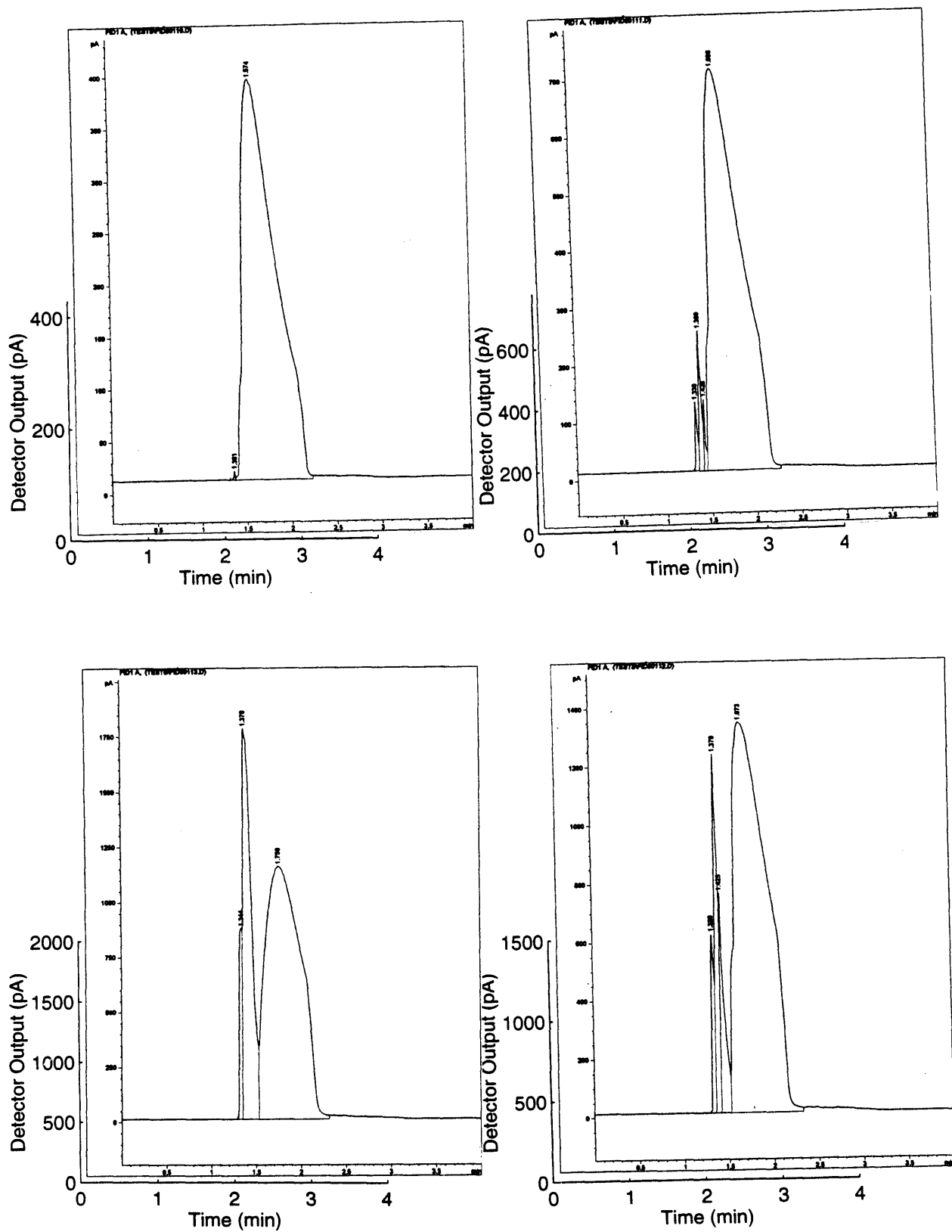


Figure 6-12: Results for injection volume variation experiments for polyethylene. Clockwise starting from the top left corner: 0.1 ml, 0.2 ml, 0.4 ml, and 0.6 ml.

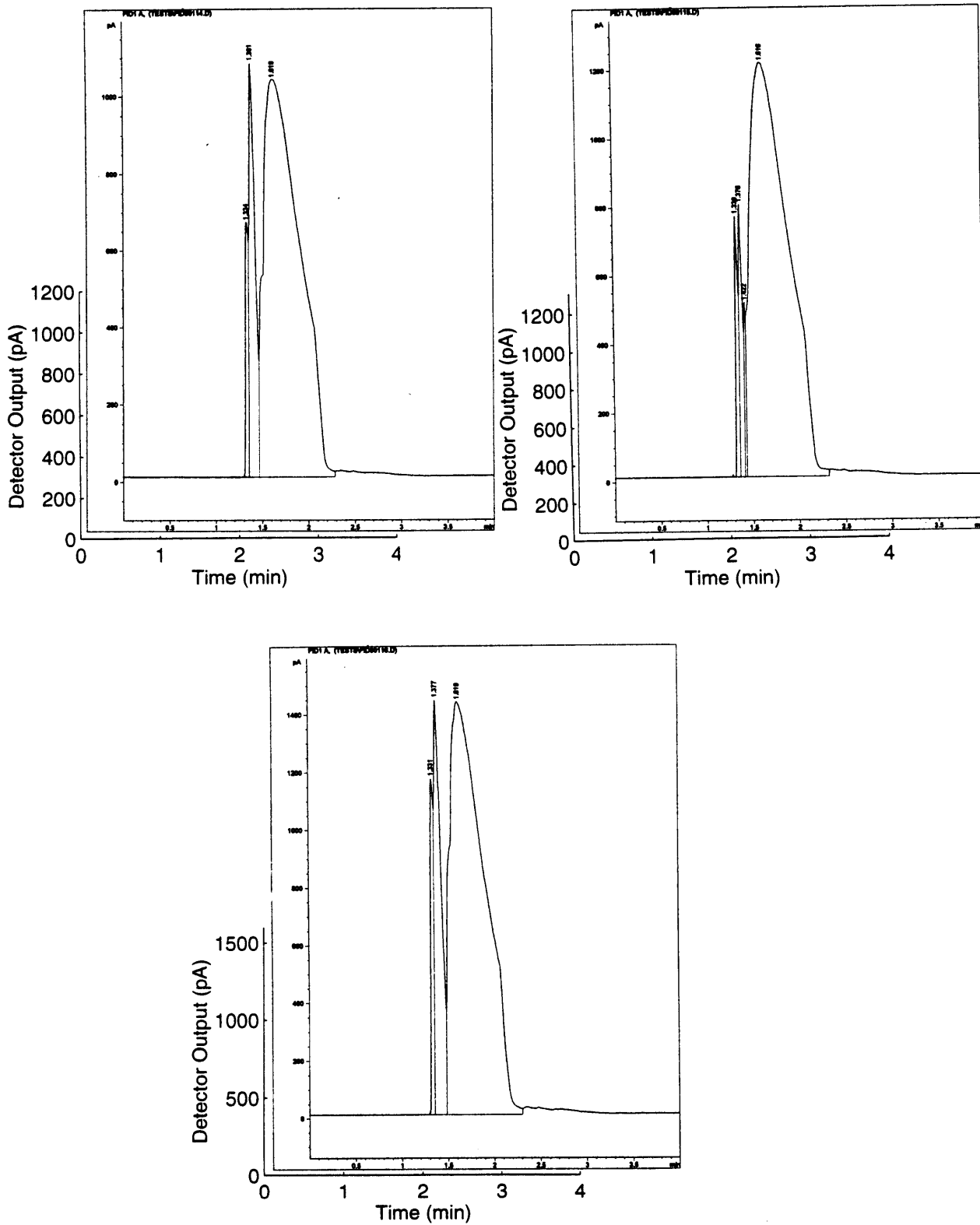


Figure 6-13: Results for ablation time variation experiments for polyethylene. Clockwise starting from the top left corner: 60 seconds, 90 seconds, and 120 seconds.

Chapter 7

Conclusion and Recommendations

It is evident that the current results are very promising in providing new tools for the development of a microanalyzer system. The micro-column manufacturing process development was successful in providing robust tubular micro-columns, in a fast, cheap, simple manner. The hollowness of the columns was observed using a light microscope and by immersion of the ends via capillary action. These micro-columns may be very useful in several applications. The excimer laser ablation experiments showed that there is potential in using the analysis of ablation products as a material characterization tool. The experimental results for the SaranWrap and polyethylene showed that there is a definite relationship between ablation product components and excimer laser pulse frequency, injection volume, and ablation time. Furthermore, these may vary according to the material being analyzed. One can envision a system that exploits these differences to come up with material characterization criteria, especially if one can carefully control the variables observed. The current results can obviously be improved. Some of the possible improvements and future work are discussed in the following section.

7.1 Recommendations

7.1.1 Micro-column Manufacturing

There are several improvements which can be made to both the quartz micro-column manufacturing process and the excimer laser ablation product analysis experiments. In terms of the micro-column manufacturing, a major improvement can be the use of better fixtures to hold the quartz columns in place. As mentioned in Chapter 6, one of the major problems in the setup was the frequent episodes of column fracture due to the deformation of the Teflon ferrules when tightening the fixture nuts. Better alignment of the fixtures may also help prevent column fracture when installing them. A possible alternative may be to implement fixtures similar to the 3-jaw universal chucks used in lathes which hold round pieces quickly as the three jaws move simultaneously and automatically center the piece. In addition, automation of some of the current setup operations may help enhance the micro-column manufacturing process. For instance, the incorporation of a feedback control system for the column drawing process may be possible by having a temperature sensor which can sense when the quartz column has reached its softening point and then signal the actuator to pull it. The actuator and laser systems can also be computer controlled. Automation may help produce more uniform micro-columns. Another improvement which can be done is to change the current setup so that the actuator lies vertically instead of horizontally. This would help reduce the sagging that the columns undergo after they begin to soften. With less sagging, misalignment of the column may be avoided as it is being pulled and uniformity of the final column can be improved. Other possible changes may include spinning of the column as it is being pulled to have more uniform heating, and position control of the actuator to be able to make micro-columns of specific lengths and diameters once it is known how these vary according to pulling rate, temperature and initial column diameter. Finally, verification of the micro-columns' hollowness and measurement of their inner diameters should be carried out using an SEM.

7.1.2 Excimer Laser Ablation Experiments

In terms of the excimer laser ablation experiments, a major improvement can be made by more careful control of the ablation, sampling and analysis processes. The ablation and sampling processes may be better controlled by allowing the ablation and sampling to somehow (e.g., computer control) take place simultaneously so that better ablation product samples can be taken and analyzed. The X-Y stepper motor stages used to hold the gas-collection cell may also be computer controlled to scan the material being ablated.

The chromatographic analysis can be improved by using a gas sampling valve instead of a gas-tight syringe because sample leakage is greatly reduced and reliable quantitative analysis can be carried out in terms of calibration and component identification. Other detectors, such as the thermal conductivity detector, and other columns may be used to detect other gases which may be present in the ablation products and to further optimize the gas separation process. The use of a mass spectroscopic system in conjunction with the gas chromatograph may be a good addition for more reliable identification of components.

7.2 Possible Applications

The components that were discussed in this thesis may very well serve as tools for a system such as the one described in chapter 3 (Figure 3-7). Of course, one can foresee other uses for these tools. For instance, the micro-columns may be part of a novel, continuous-flow gas chromatographic system that allows one to scan a region and carry out sampling and analysis. Another possibility is to carry out spatial scanning of materials using an excimer laser/micro-column system to analyze chemical compounds. The micro-columns may also be used in systems which take advantage of the different physical laws which govern micro-fluidic systems. In particular, it has been found that the reduction of liquid handling systems to the micrometer and submicrometer size range means moving into the area of small Reynolds number or laminar flow [48]. This change in the physics of the flow may allow one to take

advantage of the consequences to come up with useful devices. There are several possible devices that can be implemented. For instance, valves with no moving parts can be made by controlling the pressures to affect the flow streams. Other possibilities include the extraction of particles from flows using diffusion and mixing enhancing. Aside from these possibilities, the micro-columns have much potential aside from micro-sniffers and micro-gas chromatographic columns. These include multi-purpose gas and liquid transport channels for miniaturized devices, micropipettes, miniature heat exchangers, and microprobes to name a few.

7.3 Conclusion

In conclusion, it is clear that the miniaturization of chemical analysis technology is very promising in providing novel, smaller, better performance devices which can find use in many areas of application. The results described in this thesis are a small step in this direction, and they may provide new tools for use in future development of chemical analysis micro-systems and other areas of research.

Appendix A

Gas-Collection Cell Drawing

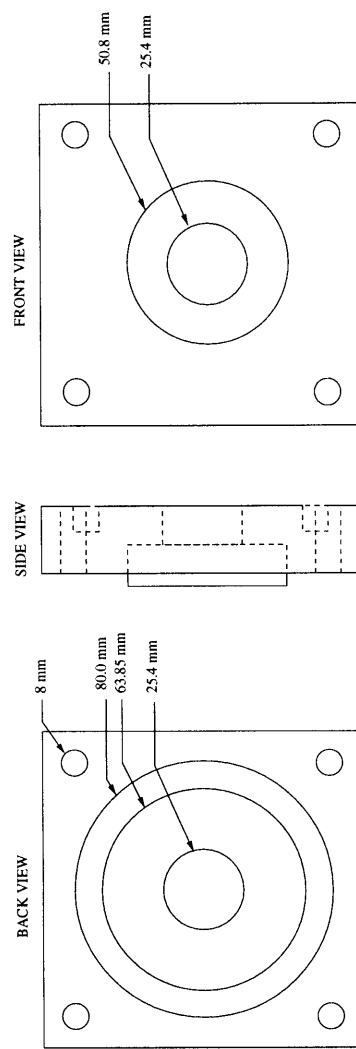


Figure A-1: Cell Drawing (Front Section).

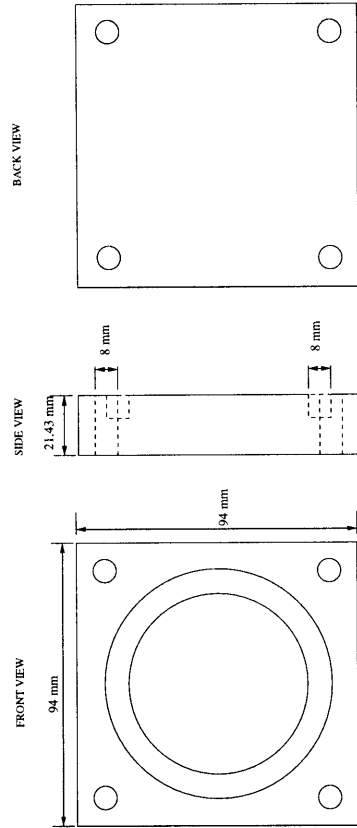


Figure A-2: Cell Drawing (Back Section).

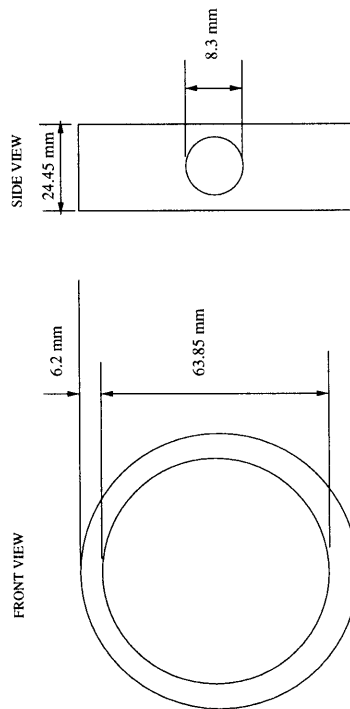


Figure A-3: Cell Drawing (Plexiglas Section).

ASSEMBLY

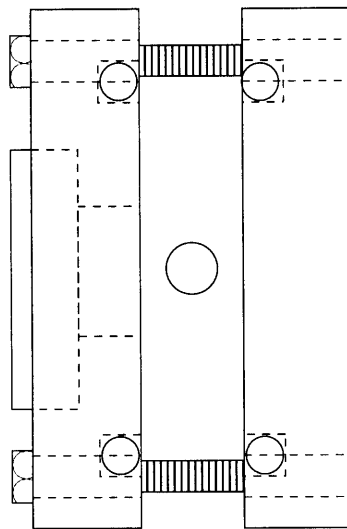


Figure A-4: Assembly Drawing.

Appendix B

Amplifier Circuit Diagram

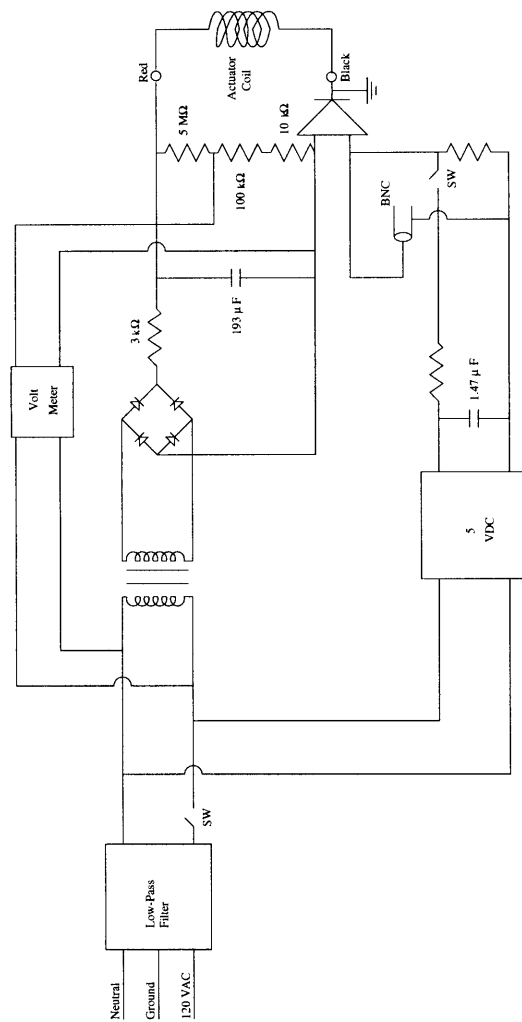


Figure B-1: Pulse Generator Circuit Diagram

Appendix C

Gas Chromatography Setpoints

The following are the settings used for the chromatographic separations using the 6890 HP gas chromatograph. The method name is REV1_AP.M.

OVEN

Initial temp: 60°C (On), Maximum temp: 320°C

Initial time: 0.00 min, Equilibration time: 0.50 min

Ramps:

No.	Rate	Final temp	Final time
-----	------	------------	------------

1	0.0 (Off)		
---	-----------	--	--

Post temp: 60°C

Post time: 0.00 min

Run time: 5.0 min

FRONT INLET

Mode: Splitless

Initial temp: 250°C (On)

Pressure: 110 kPa (On)

Purge flow: 26.6 $\frac{mL}{min}$

Purge time: 0.75 min

Total flow: 30.1 $\frac{mL}{min}$

Gas saver: On

Saver flow: $15.0 \frac{mL}{min}$

Saver time: 2.00 min

Gas type: Nitrogen

COLUMN 1

Capillary column

Model Number: HP 19091S – 433

HP – 5MS 5% Phenyl Methyl Siloxane

Max temperature: $325^{\circ}C$

Nominal length: 30.0 m

Nominal diameter: $250.00 \mu m$

Nominal film thickness: $0.25 \mu m$

Mode: constant flow

Initial flow: $1.5 \frac{mL}{min}$

Nominal initial pressure: 110 kPa

Average velocity: $36 \frac{cm}{sec}$

Inlet: Front inlet

Outlet: Front detector

Outlet pressure: ambient

FRONT DETECTOR

Temperature: $300^{\circ}C$ (On)

Hydrogen flow: $30.0 \frac{mL}{min}$ (On)

Air flow: $400.0 \frac{mL}{min}$ (On)

Mode: Constant column + makeup flow

Combined flow: $31.4 \frac{mL}{min}$

Makeup flow: On

Makeup Gas Type: Nitrogen

Flame: On

Electrometer: On

Lit offset: 2.0

SIGNAL 1

Data rate: 5 *Hz*

Type: front detector

Save Data: On

Start Save Time: 0.00 *min*

Stop Save Time: 4.00 *min*

Zero: 0.0 (Off)

Range: 0

Fast Peaks: Off

Attenuation: 0

Appendix D

Integration Results

The following tables summarize the integration results for each of the files which include each experimental result.

Retention Time	Area	Height	Width
1.379	4865.1	1291.9	0.048
1.669	31035.3	1211.3	0.304

Table D.1: File FID00095.D-Frequency rate of 10 *Hz* for SaranWrap.

Retention Time	Area	Height	Width
1.378	1168.2	645.2	0.026
1.437	270.9	195.0	0.019
1.605	31601.8	1258.3	0.306

Table D.2: File FID00096.D-Frequency rate of 50 *Hz* for SaranWrap.

Retention Time	Area	Height	Width
1.377	1495.7	1255.2	0.018
1.390	2915.4	1130.2	0.043
1.684	34475.9	1311.5	0.438

Table D.3: File FID00097.D-Frequency rate of 75 *Hz* for SaranWrap.

Retention Time	Area	Height	Width
1.380	110.6	142.7	0.012
1.396	219.2	198.2	0.016
1.618	40036.6	1524.1	0.310

Table D.4: File FID00098.D-Frequency rate of 100 *Hz* for SaranWrap.

Retention Time	Area	Height	Width
1.393	25	29.5	0.013
1.583	15244.1	595.1	0.309

Table D.5: File FID00099.D-Injection volume of 0.1 *ml* for SaranWrap.

Retention Time	Area	Height	Width
1.376	387.8	369.1	0.015
1.395	433.2	307.7	0.023
1.610	25604.3	983.2	0.434

Table D.6: File FID00100.D-Injection volume of 0.2 *ml* for SaranWrap.

Retention Time	Area	Height	Width
1.338	53.6	25.4	0.029
1.376	5956.2	1909.5	0.046
1.429	3910.4	1197.9	0.054
1.759	35001.1	1360.4	0.429

Table D.7: File FID00101.D-Injection volume of 0.4 *ml* for SaranWrap.

Retention Time	Area	Height	Width
1.384	25512.0	2702.5	0.153
1.776	37301.8	1580.1	0.393

Table D.8: File FID00102.D-Injection volume of 0.6 *ml* for SaranWrap.

Retention Time	Area	Height	Width
1.34	28.7	21.6	0.021
1.378	6545.4	1550.2	0.057
1.667	29219.4	1158.9	0.298

Table D.9: File FID00103.D-Ablation time of 60 *s* for SaranWrap.

Retention Time	Area	Height	Width
1.338	24.6	20.2	0.018
1.377	4650.6	1422.1	0.046
1.459	1133.8	430.8	0.044
1.668	28435.1	1120.2	0.336

Table D.10: File FID00104.D-Ablation time of 90 *s* for SaranWrap.

Retention Time	Area	Height	Width
1.329	23.3	11.7	0.026
1.379	1290.1	698.8	0.026
1.416	804.4	413.4	0.032
1.517	106.8 7	44.2	0.031
1.680	26191.5	1360.4	0.440

Table D.11: File FID00105.D-Ablation time of 120 *s* for SaranWrap.

Retention Time	Area	Height	Width
1.330	7.3	3.8	0.026
1.381	1300.3	661.8	0.031
1.414	1369.4	507.7	0.045
1.667	17229.4	659.0	0.310

Table D.12: File FID00106.D-Frequency rate of 10 *Hz* for polyethylene.

Retention Time	Area	Height	Width
1.330	50.9	26.1	0.027
1.381	1215.8	568.5	0.029
1.425	730.3	331.1	0.037
1.529	137.2	54.6	0.036
1.668	16717.8	660.2	0.422

Table D.13: File FID00107.D-Frequency rate of 50 *Hz* for polyethylene.

Retention Time	Area	Height	Width
1.331	163.3	81.7	0.030
1.381	1504.8	601.8	0.042
1.419	846.9	420.7	0.034
1.685	18152.4	692.1	0.317

Table D.14: File FID00108.D-Frequency rate of 75 *Hz* for polyethylene.

Retention Time	Area	Height	Width
1.332	395.5	191.2	0.031
1.381	1545.2	652.0	0.039
1.421	1019.7	425.8	0.040
1.679	20849.7	783.7	0.333

Table D.15: File FID00109.D-Frequency rate of 100 *Hz* for polyethylene.

Retention Time	Area	Height	Width
1.361	8.3	8.6	0.014
1.579	9982.9	383.6	0.315

Table D.16: File FID00110.D-Injection volume of 0.1 *ml* for polyethylene.

Retention Time	Area	Height	Width
1.331	208.5	120.8	0.024
1.380	453.0	245.2	0.026
1.425	162.6	125.6	0.018
1.606	18209.4	702.4	0.318

Table D.17: File FID00111.D-Injection volume of 0.2 *ml* for polyethylene.

Retention Time	Area	Height	Width
1.331	1346.2	605.3	0.034
1.379	3001.1	1232.8	0.041
1.425	2428.6	756.1	0.054
1.674	34696.6	1336.5	0.320

Table D.18: File FID00112.D-Injection volume of 0.4 *ml* for polyethylene.

Retention Time	Area	Height	Width
1.344	1700.3	869.9	0.033
1.378	12027.3	1776.8	0.113
1.759	31876.6	1150.6	0.327

Table D.19: File FID00113.D-Injection volume of 0.6 *ml* for polyethylene.

Retention Time	Area	Height	Width
1.336	1464.6	659.9	0.035
1.381	4694.3	1065.7	0.060
1.620	28153.4	1030.6	0.353

Table D.20: File FID00114.D-Ablation time of 60 *s* for polyethylene.

Retention Time	Area	Height	Width
1.331	1578.7	764.8	0.031
1.396	1891.9	793.3	0.032
1.423	601.8	507.5	0.017
1.616	34548.7	1207.4	0.341

Table D.21: File FID00115.D-Ablation time of 90 *s* for polyethylene.

Retention Time	Area	Height	Width
1.333	2605.9	1161.8	0.035
1.378	7404.0	1430.5	0.070
1.618	37338.8	1430.5	0.315

Table D.22: File FID00116.D-Ablation time of 120 *s* for polyethylene.

Bibliography

- [1] Janata, J. *Principles of Chemical Sensors*, New York: Plenum Press, 1989.
- [2] Consadori, F. Personal interview, August 1996, Salt Lake City, Utah.
- [3] Watson, J.T. *Introduction to Mass Spectroscopy: Biomedical, Environmental and Forensic Applications*, New York: Raven Press, 1976.
- [4] Long, D.A. *Raman Spectroscopy*, New York: McGraw-Hill, 1977.
- [5] Grasseli, J.G., Snavely, M.K. and Bulkin, B.J. *Chemical Applications of Raman Spectroscopy*, New York: Wiley-Interscience Publication, John Wiley & Sons, 1981.
- [6] Bacher, W., Menz, W., Mohr, J. The LIGA technique and its potential for microsystems, IECON '94, 20th International Conference on Industrial Electronics, Control and Instrumentation, vol. 3., 1466-71, 1994.
- [7] Stock, R., Rice, C.B.F. *Chromatographic Methods, 3rd edition*, London: Chapman and Hall, 1974.
- [8] Madou, M.J., Morrison, S.R. *Chemical Sensing with Solid State Devices*, San Diego: Academic Press, Inc., 1989.
- [9] Dibbern, U. Miniaturisation of Gas Sensor Substrate: Problems and Benefits of Microelectronic Technology, in Gardner, J.W., Bartlett, P.N. (eds.), *Sensors and Sensory Systems for an Electronic Nose*, NATO Series E: Applied Sciences, Vol. 212, ch. 10, Dordrecht; Boston: Kluwer Academic 1992.

- [10] Neaves, P.I., Hatfield, J.V. A new generation of integrated electronic noses, *Sensors and Actuators*, B, 26-27, 223-231, 1995.
- [11] Gardner, J.W., Bartlett, P.N. A brief history of electronic noses, *Sensors and Actuators*, B, 18-19, 282-290, 1994.
- [12] Stetter, J.R. Chemical sensor arrays: practical insights and examples, in Gardner J.W., P.N. Bartlett, P.N. (eds.), *Sensors and Sensory Systems for an Electronic Nose*, NATO Series E: Applied Sciences, Vol. 212, ch. 17, Dordrecht; Boston: Kluwer Academic 1992.
- [13] Carey, W.P., Yee, S.S. Calibration of nonlinear solid-state sensor arrays using multivariable regression techniques, *Sensors and Actuators*, B, 9, 112-113, 1992.
- [14] Wlodek, S., Colbow, K. and Consadori, F. Kinetic model of a thermally cycled tin oxide gas sensor, *Sensors and Actuators*, B, 3(2), 123-127, 1991.
- [15] Wlodek, S., Colbow, K. and Consadori, F. Signal shape analysis of thermally cycled tin oxide gas sensor, *Sensors and Actuators*, B, 3(1), 63-68, 1991.
- [16] Sears, W.M., Colbow, K., Slamka, R. and Consadori, F. Selective thermally cycled gas sensing using fast Fourier transform techniques, *Sensors and Actuators*, B, 2(4), 283-289, 1990.
- [17] Sears, W.M., Colbow, K., and Consadori, F. Algorithms to improve the selectivity of thermally cycled tin oxide gas sensors, *Sensors and Actuators*, 19(4), 333-349, 1989.
- [18] Skoog, D.A., West, P.M., Holler, F.J. *Fundamentals of Analytical Chemistry, Fifth Edition*, New York: W.B. Saunders Co., 1988.
- [19] Schomburg, G., *Gas Chromatography: A Practical Course*, New York: VCH Publishers, Inc., 1990.

- [20] Terry, S.C., Jerman, J.H., and Angell, J.B. A gas chromatographic air analyzer fabricated on a silicon wafer, *IEEE Transactions on Electron Devices*, Vol. ED-26, No. 12, 1880-1886, Dec. 1979.
- [21] Angell, J.B., Terry, S.C., and Barth, P.W. Silicon micromechanical devices, *Scientific American*, vol. 248, No. 4, 44, 1983.
- [22] Manz, A., Miyahara, Y., Miura, J., Watanabe, Y., Miyagi, H., Sato, K. Design of an open-tubular column liquid chromatograph using silicon chip technology, *Sensors and Actuators*, B1, 249-255, 1990.
- [23] Karube, I., Yokoyama, K. Trends in biosensor research and development, *Sensors and Actuators*, B, 13-14, 12-15, 1993.
- [24] Harrison, D.J., Glavina, P.G., Manz, A. Towards miniaturized electrophoresis and chemical analysis systems on silicon: an alternative to chemical sensors, *Sensors and Actuators*, B, 10, 107-116, 1993.
- [25] Harrison, D.J., Fluri, K., Seiler, K., Fan, Z., Effenhauser, C.S., Manz, A. Micromachining a miniaturized capillary electrophoresis-based chemical analysis system on a chip, *Science*, vol. 261, 895-897, Aug. 13, 1993.
- [26] Jacobson, S.C., Hergenroder, R., Koutny, L.B., Ramsey, J.M. Open channel electrochromatography on a microchip, *Analytical Chemistry*, 66, 2369-2373, 1994.
- [27] Jacobson, S.C., Hergenroder, R., Koutny, L.B., Ramsey, J.M. High-Speed Separations on a Microchip, *Analytical Chemistry*, 66, 1114-1118, 1994.
- [28] Jacobson, S.C., Hergenroder, R., Koutny, L.B., Warmack, R.J., Ramsey, J.M. Effects of injection schemes and column geometry on the performance of microchip electrophoresis devices, *Analytical Chemistry*, 66, 1107-1113, 1994.
- [29] Raymond, D.E., Manz, A., Widmer, H.M. Continuous sample pretreatment using a free-flow electrophoresis device integrated onto a silicon chip, *Analytical Chemistry*, 66, 2858-2865, 1994.

- [30] Jacobson, S.C., Koutny, L.B., Hergenroder, R., Moore, A.W., Ramsey, J.M. Microchip Capillary Electrophoresis with an Integrated Postcolumn Reactor, *Analytical Chemistry*, 66, 3472-3476, 1994.
- [31] Effenhauser, C.S., Manz, A., Widmer, H.M. Glass chips for high-speed capillary electrophoresis separations with submicrometer plate heights, *Analytical Chemistry*, 65, 2637-2642, 1993.
- [32] Manz, A., Graber, N., Widmer, H.M. Miniaturized total chemical analysis systems: a novel concept for chemical sensing, *Sensors and Actuators*, B1, 244-248, 1990.
- [33] Manz, A., Harrison, D.J., Verpoorte, F., Fettinger, J.C., Paulus, A., Ludi, H., Widmer, H.M. Planar chips technology for miniaturization and integration of separation techniques into monitoring systems: Capillary electrophoresis on a chip, *Journal of Chromatography*, 593, 253-258, 1992.
- [34] Mitsubayashi, K., Yokoyama, K., Takeuchi, T., Karube, I. Gas-phase biosensor for ethanol, *Analytical Chemistry*, 66, 3297-3302, 1994.
- [35] Poulin, G.D., Eisele, P.A. Advances in excimer laser materials processing, *Excimer Beam Applications*, SPIE, vol. 998, 84-89, 1988.
- [36] Moore, J.H., Davis, C.C., Coplan, M.A. *Building Scientific Apparatus, 2nd Edition*, New York: Addison-Wesley, 1989.
- [37] Srinivasan, R. Kinetics of the ablative decomposition of organic polymers in the far ultraviolet, *Journal of Vacuum Science Technology*, B1, 923-926, 1993.
- [38] Larciprete, R., Stuke, M. Direct observation of excimer-laser phototablation products from polymers by picosecond-UV-laser mass spectroscopy, *Applied Physics*, B, 181-184, 1987.
- [39] Dyer, P.E., Oldershaw, G.A., Schudel, D. XeCl laser ablation of polyetheretherketone, *Applied Physics*, B 51, 314-316, 1990.

- [40] Singleton, D.L., Paraskevopoulos, G., Jolly, G.S., Irwin, R.S., McKenney, D.J., Nip, W.S., Farrell, E.M., Higginson, L.A.J. Excimer lasers in cardiovascular surgery: Ablation products and photoacoustic spectrum of arterial wall, *Applied Physics Letters*, vol. 48, No. 13, 878-880, March 1986.
- [41] Singleton, D.L., Paraskevopoulos, G., Irwin, R.S. XeCl laser ablation of polyimide: Influence of ambient atmosphere on particulate and gaseous products, *Journal of Applied Physics* 66(7), 3324-3328, October 1989.
- [42] Franklin, G.F., Powell, J.D., Emami-Naeini, A. *Feedback Control Of Dynamic Systems, 3rd Ed.*, Reading, MA: Addison-Wesley Publishing Co., 1994.
- [43] Sutter Company Catalog, Novato, CA, October 1996.
- [44] Bolz, R.E., Tuve, G.L., Eds. *Handbook of Tables for Applied Engineering Science, 2nd ed.*, Cleveland: CRC Press, 1973.
- [45] D' Couto, G.C., Babu, S.V. Heat transfer and material removal in pulsed excimer-laser-induced ablation: Pulsewidth dependence, *Journal of Applied Physics*, 76(5), 3052-3058, September 1994.
- [46] *Consumer Reports*, p. 143., March 1994
- [47] Grob, R.L. *Modern Practice of Gas Chromatography*, New York: John Wiley & Sons, Inc., 1995.
- [48] Brody, J.P., Yager, P., Goldstein, R.E., Austin, R.H. Biotechnology at low Reynolds numbers, *Biophysical Journal*, vol. 71, 3430-3441, 1996.